5-1-2022

Reducing Torsion in Asymmetric Structures During Earthquakes Through Active Control

Keona Lauren Banks

Reducing Torsion in Asymmetric Structures During Earthquakes Through Active Control

by

Keona Lauren Banks

An Honors Capstone

submitted in partial fulfillment of the requirements

for the Honors Diploma or Certificate

to

The Honors College

of

The University of Alabama in Huntsville

5/1/2022

Honors Capstone Director: Dr. Richard Tantaris

Lecturer of Mechanical and Aerospace Engineering

Keona Banks 4/27/2022
Student (signature) Date

4/29/22
Director (signature) Date

04/29/2022
Department Chair (signature) Date

William Wilkerson Digitally signed by William Wilkerson
Date: 2022.05.01 13:56:20 -05'00'
Honors College Dean (signature) Date

HONORS COLLEGE
THE UNIVERSITY OF ALABAMA IN HUNTSVILLE

Honors College
Frank Franz Hall
+1 (256) 824-6450 (voice)
+1 (256) 824-7339 (fax)
honors@uah.edu

Honors Thesis Copyright Permission

This form must be signed by the student and submitted as a bound part of the thesis.

In presenting this thesis in partial fulfillment of the requirements for Honors Diploma or Certificate from The University of Alabama in Huntsville, I agree that the Library of this University shall make it freely available for inspection. I further agree that permission for extensive copying for scholarly purposes may be granted by my advisor or, in his/her absence, by the Chair of the Department, Director of the Program, or the Dean of the Honors College. It is also understood that due recognition shall be given to me and to The University of Alabama in Huntsville in any scholarly use which may be made of any material in this thesis.

___Keona _Banks_____

Student Name (printed)

Student Signature

__4/27/2022___

Date

Table of Contents

Dedication

Preparing this capstone would have not been possible without support of many people. I would like to acknowledge my advisor Dr. Richard Tantaris, for his support. I would also like to thank my peers who provided valuable comments and discussions which improved the quality of this work. Finally, this work would have not been possible without the support of my family and friends motivating me to strive for more.

Abstract

The following manuscript is inspired by the initial efforts of my senior design project to design a linear active base isolation system. Through this endeavor it was found that asymmetry in structures is often ignored when developing control systems for seismic protection. However, asymmetric structures are known to undergo more severe damage than their symmetric counterparts. The objective for the project is to understand the influence of asymmetries on a structure's movement and design a controller that can reduce the torsional effects. An active control system was developed using a hydraulic linear actuator and an LQR controller. The desired response parameters included a reduction in peak angular displacement of 50 percent, comparable to a passive design and similar active systems. The MATLAB Simulink controller simulations produced up to a 55 percent reduction in peak angular displacement of a single story. In addition, the lateral displacement was consequently reduced by 74 percent. While exploring the sensitivity of the controller to various system properties, it was discovered the most influential parameter was the position of the actuator, offering more torque control with increasing offset from the center of mass.

Introduction

Base isolation, shear walls, and cross-braces are all standard techniques to earthquake-proof a building, but buildings can be smarter. Smart structures sense changes to the environment and respond in real time with the aid of an active or semi-active control system. One such example is Yokohama Landmark Tower built in 1993 Tokyo, Japan. The building boasts a hybrid control system that combines a tuned spring system and an AC servomotor (Yamazaki, et. al 1992). Installed on the first floor of the penthouse 282 meters from the ground, the system reduces wind-induced swaying by a factor of twelve (Yamazaki, et. al 1992). A hot spot for severe seismic activity, Japan overall is wonderful case study on seismic protective strategies and technology.

The United States, by contrast, lacks implementation of earthquake protective measures overall, let alone full-scale active seismic control. One reason for this is the tradeoff between up-front prevention and future repair cost. Buildings are made to be rebuilt not to be resilient. A 2018 U.S. Geological Survey “The Hayward Earthquake Scenario” found that a quarter of the buildings in San Francisco Bay Area, home to about 8 million residents, would not be functional after a magnitude 7 earthquake (Hudnut et. al. 2018). The same study predicts such an event is expected in the next 50 years. Stricter seismic regulations and control systems necessitate higher up-front costs and longer completion times but could also save billions of dollars in damage.

Torsional irregularities are one of the major causes of structural failure during earthquakes. Buildings with asymmetrical designs are subject to amplified rotational motion and experience much greater damage than their symmetrical counterparts (Özmen, et. al.

2014). This project aims to design a control system that will reduce the torsional response of an asymmetric structure with the broad goal of exploring a fascinating application of control design.

Chapter 1: A Literature Review

A Discussion on Key Concepts:

Although structural design is a subset of civil engineering, a knowledge of earthquakes and control systems are also necessary to approach seismic design problems. There are terms and assumptions that are standard within the specialty that are not inherently obvious. From a mechanical engineering perspective, this is a brief discussion on concepts that I learned through the journey of this project and consider valuable to the understanding of the overall work.

One of the fundamental concepts taught in structural engineering is strong column-weak beam design. Strong column-weak beam design requires, as the name suggests, columns should be stiffer than beams. The criteria are important because if a beam were to fail, one story would collapse, but if a column were to fail, an entire structure will fall. The concept is incorporated into numerous international building codes as a standard approach to prevent total structural failure (Nie, et. al. 2020). It is particularly necessary in seismic design to ensure the building can resist strong horizontal forces during an earthquake. Therefore, when deriving a mathematical representation for a building, it is practical to estimate structural stiffness from column properties as long as columns are designed to be the main contributors to building stiffness.

Damping is a more complex property to mathematically derive than stiffness. In fact, the prediction of numerical damping values is an ongoing controversy in structural design and there is no one preferred technique (Kijewski and Kareem 2000). The macroscopic and microscopic behavior of materials, architectural design, friction between members and joints, and air resistance are each a source of damping. Each dissipates energy from a building. Of the many

phenomena that facilitate energy dissipation, experiments have shown displacement-based friction influences the damping behavior of a building most (Kijewski and Kareem 2000)(Alipour and Zareian 2008). Akin to when stiffness is estimated from column properties, it is reasonable to estimate damping from friction. However, a friction-based mathematical model requires a nonlinear analysis. An alternative and standard engineering practice is to represent a building's damping values through the Rayleigh model, a viscous damping model that states damping is a value proportional to stiffness and mass (Alipour and Zareian 2008). The Rayleigh model is linear and therefore more convenient to implement when developing equations of motion, but it will not capture the full behavior of a system and its nonlinearities.

The third fundamental idea to consider is center of rigidity (CR) and how it relates to the center of mass (CM). The center of rigidity is more prevalent in civil engineering than mechanical engineering and is often in reference to a floor plan. The CR is where stiffness is concentrated and is where resistive forces act. It can be described as the point where the structure will not rotate when a lateral force is applied. For comparison, the CM is a point where mass is concentrated and is where inertial loads act. As buildings are structures of mixed materials and complex design, the CR and CM are often idealized to sit at the same location. The true distance between the points is known as eccentricity. During an earthquake, inertial forces are induced at the CM and the building resists deformation about the CR, resulting in rotation equivalent to the eccentricity times the applied force. If the focus of an analysis is a translational motion, this moment can be neglected. It is imperative not to make that assumption when torsional damage is a concern.

How Engineers Tackle Asymmetry and Torsion:

An early defense against torsional damage is to minimize asymmetry in the initial building design. To strive for complete symmetry, however, is unrealistic due to functional and architectural demands. In theory, designs can be optimized during the initial planning stages of construction with the use of mathematical models to predict building behavior. In 2020, researchers Botis and Cerbu developed a theoretical approach to minimize eccentricity by adjusting column sizes iteratively (Botis and Cerbu 2020). The proposed approach depends on the accuracy of behavioral predictions and emphasizes the lack of literature that tackles the mathematical analysis of asymmetric structures and torsion, inviting further research.

Seismic design approaches can be organized into three categories: passive, hybrid, and active systems. A diagram of common earthquake protective measures in each category are shown in Figure 1. The most popular passive approach is base isolation which involves decoupling a foundation from a structure to divert energy from the ground. A close second in popularity and newer in development are tuned mass dampers (TMD), which use a mass to absorb seismic energy from the structure (Fisco and Adeli 2011). Tuned mass dampers are found to be effective against a narrow range of seismic frequencies. Through theoretical formulation, Villaverde and Koyoama demonstrated that a TMD can reduce peak displacements in a ten-story building by about 38 percent against random excitation (Villaverde and Koyama 1993). When exploring torsional responses, typical tuned mass dampers were not as effective for irregular structures under strong ground motion, especially when multiple frequencies dominate the response of the building.

In the last couple of decades, active control systems have been implemented to further optimize overall seismic design against less predictable events. Active systems include a sensor, actuator, and a control device. Active tuned mass dampers (AMTD) were one of the first implementations of active seismic design in the early 2000s. This is demonstrated by Lee and Wang in 2004. The researchers adjusted the pitch of a ball screw to control the movement of a five-story building and demonstrated proper tuning could lead to up to 70 percent reduction in peak amplitudes (Lee and Wang 2004). They also warned that if the pitch was not tuned properly it would lead to significant damage to the building. Additional limitations to be aware of include the utility requirements needed to maintain an actuator and the force requirements needed to counteract the movement of a multi-story structure. Early in practical development in the United States there are clear paths for further research. Active seismic control is an attractive idea to retrofit existing structures and protect them against a wide range of excitations. As mathematical models evolve and improve in the field, the ability to anticipate structural damage will improve, as well.

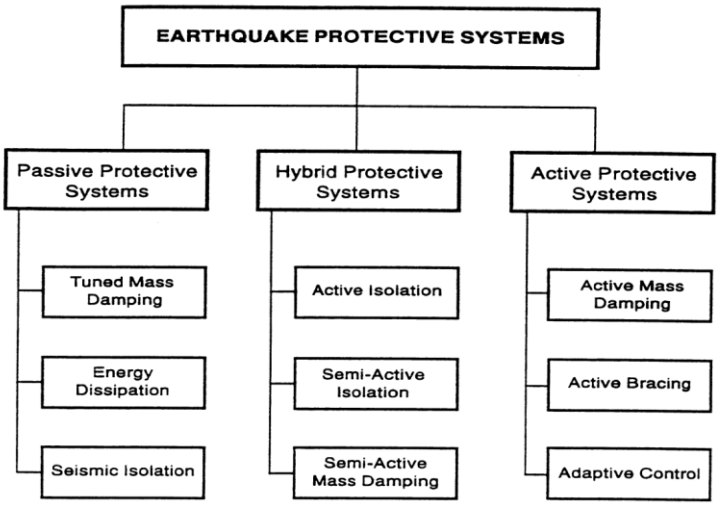

Figure 1 Family of Protective Control Systems (Mevada and Jangid 2012)

Modeling and Control Approaches:

The standard approach to mathematically modeling a multi-story building involves simplifying each level as a single lumped mass. The mass-spring-damper model is the overwhelming choice for representing the dynamics of a building whether it is asymmetrical or symmetrical (Buckle 2000)(Braz-César, et. al. 2018). When representing floors of irregular buildings, a floor plan can be simplified to two degrees of freedom instead of three. This is when eccentricity is measured along one axis of direction (Buckle 2000) (Mehana, et. al. 2019). In this approach, only two second-order linear equations are needed per story of a structure.

Once equations of motion are derived for the movement of each floor, the response can be incorporated into a theoretical control design that will adjust a building to a desired response. Recent studies are implementing fuzzy logic controllers in active seismic design. Three more prominent control designs are Proportional-Integral-Derivative (PID) control, Linear-Quadratic Regulator (LQR) control, and hybrid variations of the two (Yan, et. al. 2020), (Baygi and Karsaz 2018)]. Both PID and LQR control designs implement feedback loops. Feedback controller design detects the response of a system and feeds it back into the input of the system to adjust for error. In the context of an asymmetric building, the monitored response could be the rotational displacement from an initial zero position. Error is then adjusted by a gain to improve the actuator response. A more detailed overview of control theory will be introduced in Chapter 4 but one key difference to note is how LQR and PID control approach gain. Overall, LQR has shown better control than PID when reducing torsional motion in multiple studies while other approaches such as fuzzy logic controllers are

theoretically promising (Yan, et. al. 2020) (Baygi and Karsaz 2018)(Buckle 2000),(Braz-César, et. al. 2018).

Conclusions

The field of active control as it pertains to seismic design is young, a couple of decades old compared to centuries of passive seismic design techniques. However, it is a growing and exciting field with practical applications. This project will follow the typical method of deriving equations of motions for an asymmetrical structure as has been implemented in all papers cited. Similar to how Bertis and Cerbu reduced asymmetry through modifying column properties, a building model with intentional asymmetry can be formed in this way. The control design of interest will be an LQR controller with a hydraulic linear actuator. The accuracy of the model will be limited by assumptions such as those needed to estimate damping and stiffness properties. A question to explore is how dramatically the performance of the controller is affected by the accuracy of the eccentricity approximations. The second question to explore is how control improves with various placements of the actuator.

Chapter 2: System Math Models

A Building Model:

The floor plan illustrated in Figure 2 reflects the chosen layout of a single-story that will be implemented into the control design. The floor plan was given a simple rectangular layout of width b and length a. An asymmetrical distribution of columns, illustrated as grey squares, introduces non uniform stiffness. They introduce eccentricity,e_x, in the x-direction. Notice how columns have a larger cross-sectional area on the right than on the left. The column configuration results in a stiff edge near the larger columns and a flexible edge near the smaller columns. Therefore, the center of mass and center of rigidity will vary solely in the x direction. The equations of motion can be written for translation in the y-direction and rotation about the central z-axis, which points out of the page.

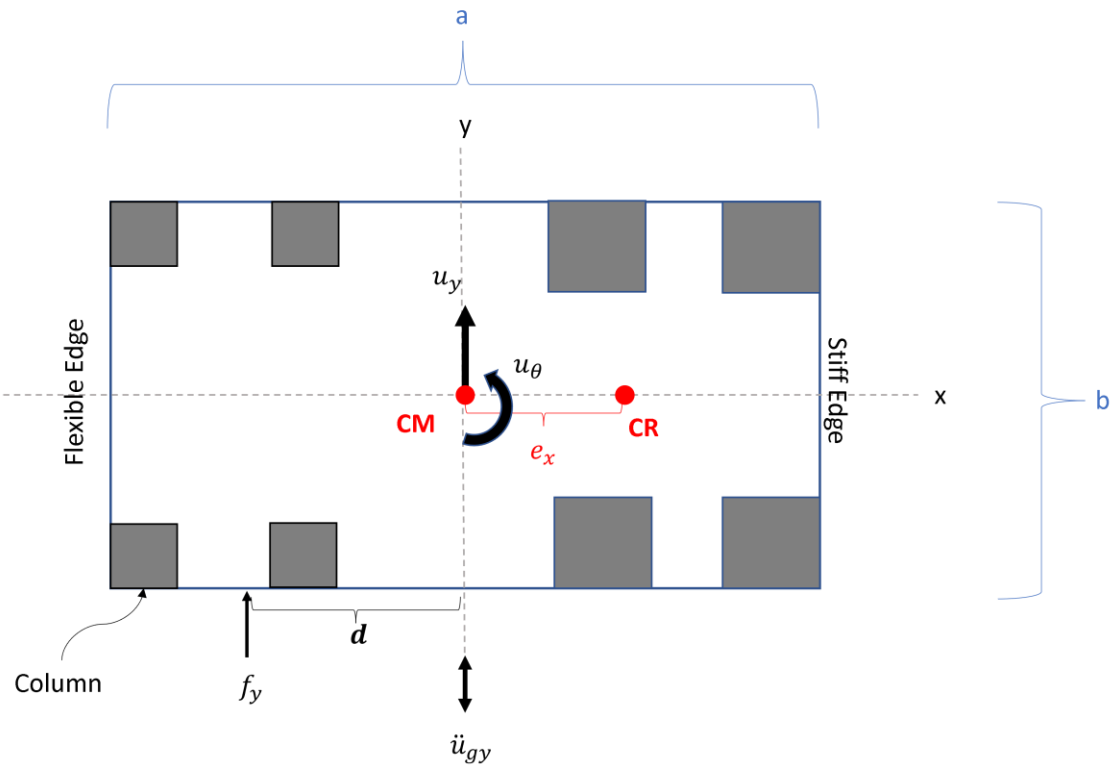

Figure 2. Floor plan of building model subject to ground acceleration $\ddot{u}_{gy}$

An actuating force acts some distance, d, to the left of the center of mass, closer to the flexible edge. In this way, the actuator can produce a torque that opposes inherent rotational response of the floor plan. With these assumptions, a single floor can be modeled with two degrees of freedom. One degree of freedom is a lateral translation, u_y while the second is torsional rotation, u_θ. Note that because the ground movement is applied in one direction the building is assumed to translate in that same lateral direction, as well.

Equations of Motion for a Single-Story:

The dynamics of the floor plan can be mathematically represented with a linear and rotational mass-spring-damper model. The linear dynamics of the building are the summation of the inertia, internal forces relative to damping and velocity, and internal forces relative to stiffness and displacement. The ground force of an earthquake and actuator force will be applied on the right-hand side of the equation.

$$F_{inertial} + F_{damping} + F_{stiffness} = -F_{ground} + F_{actuator}$$

…

$$m\ddot{u} + c(\dot{u}_y + e_x\dot{u}_\theta) + k_y(u_y + e_x u_\theta) = -m\,\ddot{u}_{gy} + f_y$$

The rotational response is represented by the sum of the torque due to the mass moment of inertia, torque relative to damping and angular velocity, and torque relative to stiffness and angular displacement. Any rotational response induced by ground acceleration and the torque produced the actuating force are on the right-hand side of the equation.

$$T_{inertial} + T_{damping} + T_{stiff} = -T_{ground} + T_{actuator}$$

…

$$I\ddot{u}_\theta + c(e_x\dot{u}_\theta + r_g^2\Omega_\theta^2\dot{u}_\theta) + k_y(e_x u_y + r_g^2\Omega_\theta^2 u_\theta) = -I\,\ddot{u}_{gy} + f_y d$$

Both equations can be organized into a matrix representation of the mass spring damper model.

$$\boldsymbol{M\ddot{u} + C\dot{u} + Ku} = -\boldsymbol{M}\ \ddot{u}_{gy} + \boldsymbol{\Gamma} f_y$$

where **M** is the mass matrix, **C** is the damping matrix, and **K** is the stiffness matrix. The position vector $\boldsymbol{u}$ encompasses the rotational and translational position variables. Then, the overall system response is equal to the external forces applied by ground acceleration $\ddot{u}_{gy}$ and an opposing control force f_y . The coefficient vector $\boldsymbol{\Gamma}$ describes the influence of the control force on each degree of freedom. With two degrees of freedom, the first row of the matrices describes translational movement while the second row of the matrices describes rotational movement about the center of mass.

$$\boldsymbol{u} = \begin{bmatrix} u_y \\ u_\theta \end{bmatrix}$$

$$\Gamma f_y = \begin{bmatrix} 1 \\ d \end{bmatrix} f_y$$

Similarly, the first and second column of the stiffness and damping matrices represents translation and rotation. The $u_y, \ddot{u}_{gy}, and\ f_y$ are displacement, ground acceleration, and actuating force in the y direction, respectively. The u_θ and T are angular position and actuating torque about the center of mass. The mass matrix contains, m, the mass and I, the mass moment of inertia, for the floor plan.

$$\boldsymbol{M} = \begin{bmatrix} m & 0 \\ 0 & I \end{bmatrix}$$

The mass moment of inertia can be calculated by treating the floor as a thin plate, where a is length and b width of the floor plan.

$$I_{thin\ plate} = \frac{1}{12} m(a^2 + b^2)$$

The mass moment of inertia is also equivalent to the mass times the square of the radius of gyration.

$$\mathrm{I} = mr_g^2$$

Where the radius of gyration could be solved from the thin plate equivalent,

$$r_g = \sqrt{\frac{a^2 + b^2}{12}}$$

The stiffness matrix is written as,

$$\boldsymbol{K} = k_y \begin{bmatrix} 1 & e_x \\ e_x & r_g^2 \Omega_\theta^2 \end{bmatrix}$$

Where k_y is the lateral stiffness in the y direction, e_x is the eccentricity in the x-direction, and Ω_θ is the ratio of the torsional frequency, ω_θ, and translational frequency, ω_y,

$$\Omega_\theta = \frac{\omega_\theta}{\omega_y}$$

The natural frequencies are found by,

$$\omega_\theta = \sqrt{\frac{k_{\theta r}}{I}}$$

$$\omega_y = \sqrt{\frac{k_y}{m}}$$

Where $k_{\theta r}$ is the rotational stiffness about the center of rigidity which is equivalent to the rotational stiffness about the center of mass shifted by the eccentricity using the parallel axis theorem. The parallel axis theorem applies to stiffness when treating lateral stiffness like mass and rotational stiffness like mass moment of inertia.

$$k_{\theta r} = k_{\theta\theta} - e_x^2 k_y$$

In addition, the rotational stiffness is computed as the sum of rotational stiffness due to the x and y positions of the center of mass,

$$k_{\theta\theta} = k_x y^2 + k_y x^2$$

Finally, the damping properties of a building are not simple to obtain and are estimated as proportional to the mass and stiffness by some constants λ and μ. The constants are derived through a modal analysis shown in Chapter 3.

$$\boldsymbol{C} = \lambda \boldsymbol{M} + \mu \boldsymbol{K}$$

$$\boldsymbol{C} = \begin{bmatrix} \lambda m + \mu & \mu e_x \\ \mu e_x & \lambda I + \mu r_g^2 \Omega_\theta^2 \end{bmatrix}$$

State Space Represenation:

Now, to derive the state space representation of the matrix form of the equations of motion. The equations of motion can be solved into the state space form with the ground motion represented as a disturbance, also referred to as an exogenous input,

$$\dot{\boldsymbol{Z}} = \boldsymbol{A}\boldsymbol{Z} + \boldsymbol{B} f_y + \boldsymbol{E}\ddot{u}_{\boldsymbol{gy}}$$

Where the state vector is defined as,

$$\boldsymbol{Z} = \begin{bmatrix} \boldsymbol{u} \\ \dot{\boldsymbol{u}} \end{bmatrix} = \begin{bmatrix} u_y \\ u_\theta \\ \dot{u}_y \\ \dot{u}_\theta \end{bmatrix}, \ \dot{\boldsymbol{Z}} = \begin{bmatrix} \dot{\boldsymbol{u}} \\ \ddot{\boldsymbol{u}} \end{bmatrix} = \begin{bmatrix} \dot{u}_y \\ \dot{u}_\theta \\ \ddot{u}_y \\ \ddot{u}_\theta \end{bmatrix}$$

Remember the matrix form of the equations of motion are,

$$\boldsymbol{M}\ddot{\boldsymbol{u}} + \boldsymbol{C}\dot{\boldsymbol{u}} + \boldsymbol{K}\boldsymbol{u} = -\boldsymbol{M}\ \ddot{u}_{\,gy} + \boldsymbol{\Gamma} f_y$$

Therefore, the equations for the state variables can be written where the highest order derivative term is isolated on the left-hand side,

$$\dot{\boldsymbol{u}} = \boldsymbol{I}\dot{\boldsymbol{u}}$$

$$\ddot{\boldsymbol{u}} = -\mathbf{M}^{-1}\boldsymbol{C}\dot{\boldsymbol{u}} - \mathbf{M}^{-1}\boldsymbol{K}\boldsymbol{u} - \mathbf{1}\,\ddot{u}_{gy} + \mathbf{M}^{-1}\boldsymbol{\Gamma} f_y$$

Where $\mathbf{1}$ is a 2x1 one's matrix. Only looking at the coefficients for the state variables the A matrix is written as,

$$\boldsymbol{A} = \begin{bmatrix} \mathbf{0} & \boldsymbol{I} \\ -\boldsymbol{M}^{-1}\boldsymbol{K} & -\boldsymbol{M}^{-1}\boldsymbol{C} \end{bmatrix} = \begin{bmatrix} 0 & 0 & 1 & 0 \\ 0 & 0 & 0 & 1 \\ -1/m & -e_x/m & \lambda+\mu/m & \mu e_x/m \\ -e_x/I & -r_g^2\Omega_\theta^2/I & \mu e_x/I & \lambda+\mu r_g^2\Omega_\theta^2/I \end{bmatrix}$$

The input to the system is the actuating force, f_y. Looking only at the coefficients of the input variable, the B matrix can be written as,

$$\boldsymbol{B} = \begin{bmatrix} \mathbf{0} \\ \boldsymbol{M}^{-1}\boldsymbol{\Gamma} \end{bmatrix} = \begin{bmatrix} 0 \\ 0 \\ 1/m \\ d/I \end{bmatrix}$$

Finally, the disturbance is ground acceleration, $\ddot{u}_{gy}$, and the coefficients for disturbance in the equations of motion are organized as,

$$\boldsymbol{E} = -\begin{bmatrix} 0 \\ 0 \\ 1 \\ 1 \end{bmatrix}$$

To describe the output, the output vector **Y** of the system can then be represented in the form,

$$\boldsymbol{Y} = \boldsymbol{C}\boldsymbol{Z} + \boldsymbol{D}f$$

LQR is a full-state feedback control design that requires feedback of all state variables. Therefore, the output vector is set equal to the state vector,

$$\boldsymbol{C} = \boldsymbol{I},\ \boldsymbol{D} = 0, \therefore \boldsymbol{Y} = \boldsymbol{Z}$$

The state space model of the building was created in MATLAB Simulink as shown in Figure 3.

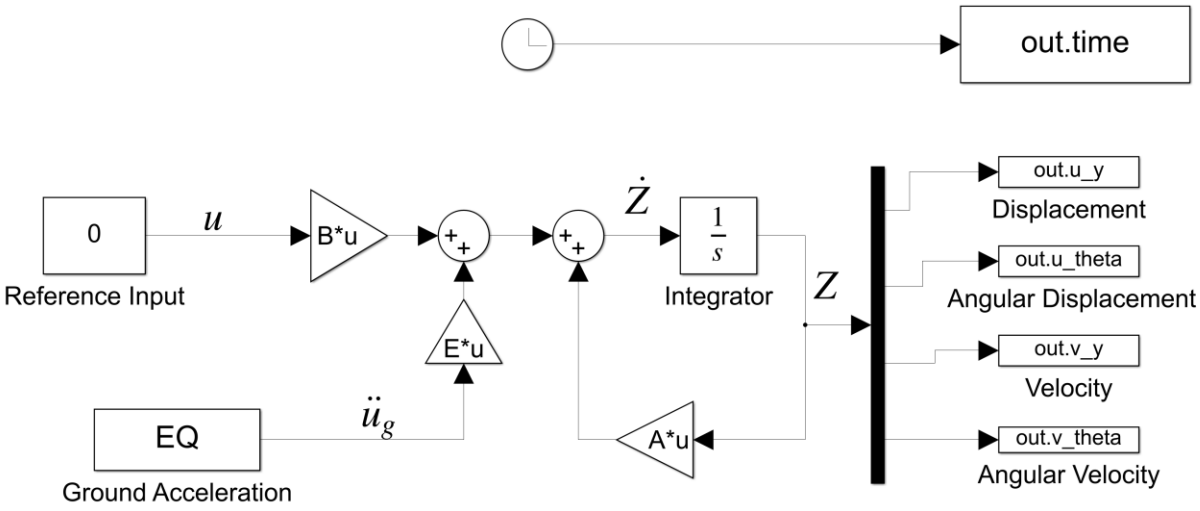

Figure 3. Open loop Simulink block diagram of building model

An Actuator:

A hydraulic linear actuator was chosen because it can produce large forces capable of shifting buildings with high speed. A general diagram of the system is pictured in Figure 4. The system takes the electrical signal of the controller to open or close a servo valve on the hydraulic actuator. The servo valve controls the flow rate of fluid into the fluid chamber. Pressure developed by the incompressible fluid drives a piston.

As seen in the equations of motion for the structure, the torsional response is coupled to the translational response. If the building translation reduces, so should rotation. In addition, the linear actuator will be offset from the center of mass by a distance equivalent to the center of rigidity to create a torque. This torque should counteract the torsional response of the building more directly.

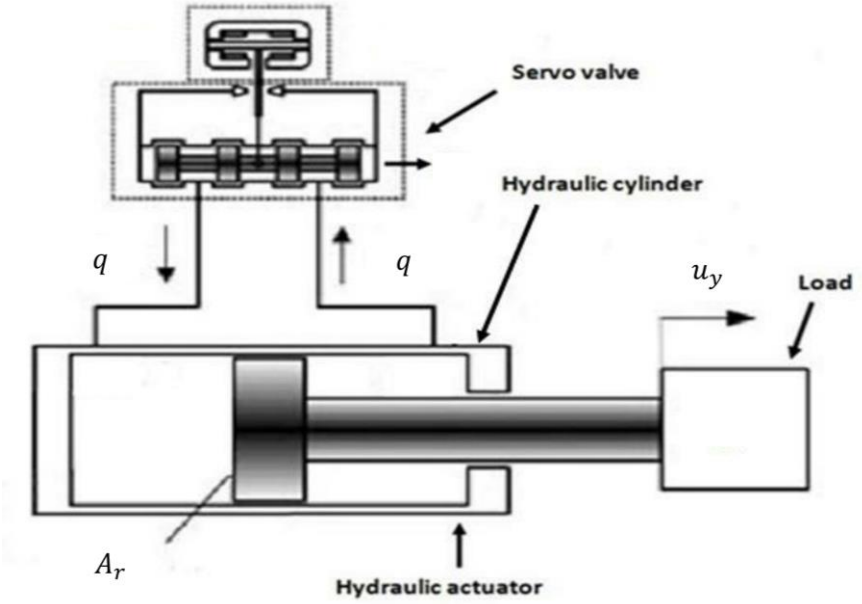

Figure 4 Diagram of a Linear Hydraulic Actuator

The hydraulic actuator dynamics can be represented by two equations to make a linearized model (DeSilva 1989). One equation describes the servo valve, and one describes the piston. The linearized equation for the fluid flow of the fluid through the valve is,

$$\frac{\tau}{g_{sv}}\dot{q} + \frac{1}{g_{sv}}q = r$$

Where τ is the servo valve time constant, g_{sv} is the servovalve, and r is the control signal. The piston dynamics are written as,

$$A_r\dot{u}_y + \frac{C_L}{A_r}f_y + \frac{V}{2C_C A_r}\dot{f}_y = q$$

Where A_r is the area of the piston, V is the volume of the fluid chamber, C_L is the leakage coefficient, C_C is the compressibility coefficient. Note that the velocity of the building $\dot{u}_y$ feeds back into the dynamics of the piston and must be accounted for in the dynamics.

Next the transfer functions for each equation will be derived. The servo valve equation in the Laplace domain assuming zero initial conditions is written as,

$$\frac{\tau}{g_{sv}}\mathrm{sQ(s)} + \frac{1}{g_{sv}}Q(s) = R(s)$$

Knowing flow rate is the output and the control signal is the input, divide over the appropriate variables and the transfer function becomes,

$$\frac{Q(s)}{R(s)} = \frac{g_{sv}}{\tau s + 1}$$

The equation for the piston is written in the Laplace domain as,

$$A_r s U_y(s) + \frac{C_L}{A_r}\mathrm{F_y(s)} + \frac{V}{2C_C A_r}\mathrm{sF_y(s)} = Q(s)$$

Knowing the force $F_y(s)$ is the output and flow rate $Q(s)$ from the servo valve is the input, the building response is ignored to form the transfer function,

$$\frac{F_y(s)}{Q(s)} = \frac{A_r}{\frac{2C_c}{V}s + \frac{1}{C_L}}$$

The Simulink Model in Figure 5 illustrates how the hydraulic actuator was implemented into the system. The transfer function for the servo valve was included in the block labeled 'Servo Valve' and the transfer function for the piston was included where the block says 'Piston.' Saturation blocks were included to represent the maximum flow and maximum force capabilities of the system. Also, note the natural velocity feedback is included in the overall diagram although it was temporarily ignored to form the piston transfer function.

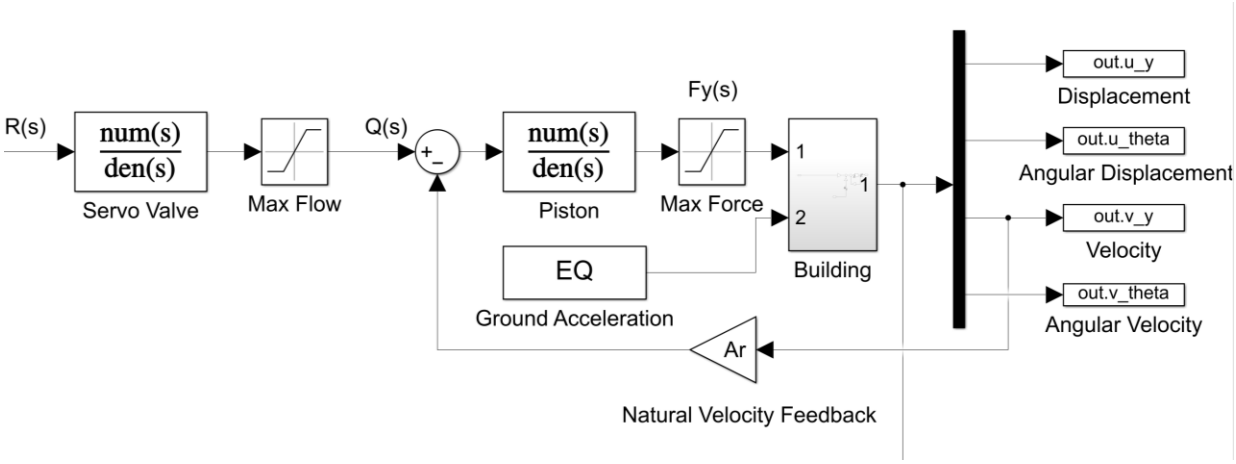

Figure 5 Linear Hydraulic Actuator in Simulink

A Sensor:

A unique challenge to active seismic control is obtaining an absolute measurement of movement. For example, to measure linear displacement or velocity, ground cannot be a reference point because the ground is moving. In fact, earthquakes disturb everything connected to ground. A common approach is to employ accelerometers at key sections in a structure and derive position and velocity through integration. One point of caution is that integrating the accelerometer readings causes noisy data that necessitates a filter. For the purposes of this project, a theoretical approach to seismic control design, the sensor will be modeled as one to represent one-to-one input and output of building response variables, assuming a highly accurate sensor system is employed.

Chapter 3: Understanding Dynamics of the System

Summary of Building Materials and Dimensions:

Characteristics about the building must be defined to implement the equations of motion and derive important values such as eccentricity or radius of gyration. The model's floor plan was created with the design criteria of the Residential Building Code 2015 in mind. This design criteria are an amended version of the International Residential Code 2015 (IRC 2015) and provided a realistic guideline for the materials and dimensions (ICC 2015). The design decisions for the model are summarized in Table 1. Note that dead load refers to permanent loads like the weight of the structure. Live load refers to temporary loads such as the inhabitants of the building or snow accumulation on the roof.

Low to mid-story structures have similar standard column and beam sizes. In seismic design there is often a tradeoff between strength and ductility. The column and beam sizes will be based on a 2015 case study that evaluated the seismic performance and resilience of an eight-story hospital in a zone with high seismic activity (Mahini, et. al. 2015). For reinforced concrete (RC) frames, steel braces were designed to support a quarter of the lateral load. The compressive strength of the concrete is assumed as 40 N/mm^2 and the yield stress of the steel is set as 340 N/mm^2 (Mahini, et. al. 2015). Note how this fulfills the strong column-weak beam design.

Table 1 Summary of System Design Details Based on Building Codes

Model Detail	**Code**	**Summary**	**Design Choice**
Column height, h	R305.1 R301.3	Habitable spaces should have a ceiling height of at least 7 feet (2.134 meters). The story height should not exceed about 11 feet for wind and seismic provisions.	3 meters
Floor width, a	R304.1	Habitable rooms should be at least 70 square feet (6.5 square meters)	6 meters
Floor length, b			8 meters
Floor Material	R402.3.1,	Materials used to produce precast concrete foundations shall have min compressive strength of 5000 psi.	Precast Concrete
Live Roof Load	R301.6	For a flat or low slope roof with less than 200 loaded area per column the minimum live roof load is 20 lb. per square foot (.958 kN per square meter)	1 kN per square meter
Floor Load	R301.5	For non-sleeping rooms account for 40 pounds per square foot (1.92 kN per square meter)	2 kN per square meter

Table 2 Summary of Column and Beam Supports

	Small Columns	Large Columns	Beams
Dimensions	180 mm x 220 mm	360 mm x 440 mm	230 mm x 180 mm
Type	Rectangular RC	Rectangular RC	Rectangular RC

Finite Element Analysis with ETABS:

Two software programs were considered for the general finite element analysis of the system: MSC Patran and CSI ETABS. MSC Patran is a more general-use program and is widely known in engineering. CSI ETABS is an engineering software specifically designed for structural analysis and it is more popular within structural design. After initial attempts modeling in MSC Patran and completing the literature review, it was determined that CSI ETABS was a more streamlined software for this system. Specifically, the CSI ETABS organization and tools of the analysis results were more relevant and user friendly for the building design. The version used for this project is CSI ETABS Ultimate 20.0.1. The floor plan of Figure 2 was recreated with properties and dimensions from Table 1 and Table 2. See the Appendix for the settings that lead into Figure 6. Figure 6 demonstrates the floor view on the left and isometric view on the right. The number of floors was an arbitrary choice since the focus of the project is controlling the response based on movement of one floor in the structure.

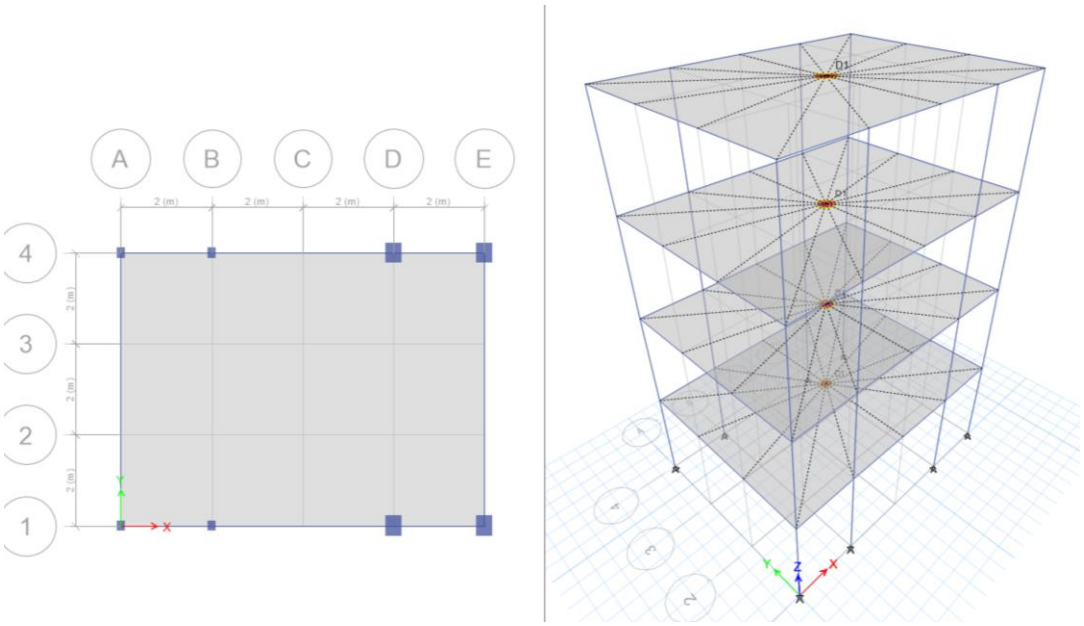

Figure 6 CSI ETABS Four-Story Model of Floor Plan

A seismic load was assigned to visualize the response of the structure and analyze key properties such as the center of rigidity and level stiffness. The deformation of the structure is illustrated in Figure 7.

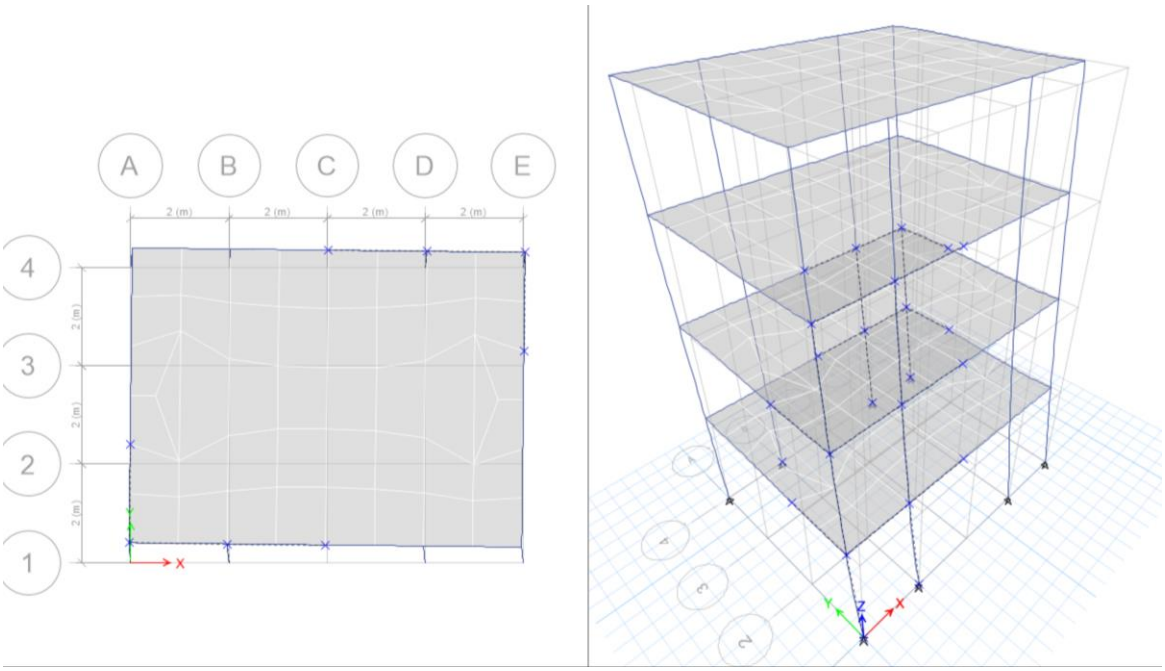

Figure 7 CSI ETABS Structural Seismic Response

Modal and Structural Analysis Results:

A modal analysis provides an overview of how the building naturally responds in the frequency domain. Each floor has three degrees of freedom and therefore contributes three modes. The modes and frequencies are tabulated in Figure 8. In addition to the modal analysis, the structural analysis calculated the center of rigidity, center of mass, and mass of each floor shown in Figure 9.

TABLE: Modal Periods And Frequencies					
Case	Mode	Period	Frequency	CircFreq	Eigenvalue
		sec	cyc/sec	rad/sec	rad²/sec²
Modal	1	1.321	0.757	4.7565	22.624
Modal	2	0.933	1.072	6.7347	45.3556
Modal	3	0.79	1.266	7.9539	63.265
Modal	4	0.28	3.566	22.4042	501.9482
Modal	5	0.232	4.302	27.0301	730.627
Modal	6	0.179	5.579	35.0512	1228.5835
Modal	7	0.121	8.278	52.0148	2705.5373
Modal	8	0.103	9.752	61.2759	3754.7327
Modal	9	0.072	13.806	86.7479	7525.2051
Modal	10	0.07	14.271	89.6663	8040.0507
Modal	11	0.059	16.94	106.4367	11328.7774
Modal	12	0.039	25.873	162.567	26428.0211

Figure 8 CSI ETABS Modal Periods and Frequencies Results

TABLE: Centers Of Mass And Rigidity											
Story	Diaphragm	Mass X	Mass Y	XCM	YCM	Cum Mass X	Cum Mass Y	XCCM	YCCM	XCR	YCR
		kg	kg	m	m	kg	kg	m	m	m	m
Story4	D1	16835.03	16835.03	4.2931	3	16835.03	16835.03	4.2931	3	4.6434	3.0005
Story3	D1	19689.52	19689.52	4.5116	3	36524.56	36524.56	4.4109	3	4.9791	3.0005
Story2	D1	19689.52	19689.52	4.5116	3	56214.08	56214.08	4.4461	3	5.3782	3.0004
Story1	D1	19689.52	19689.52	4.5116	3	75903.61	75903.61	4.4631	3	5.8705	3.0003

Figure 9 CSI ETABS Mass, CM, and CR Results

Stiff X	Shear Y	Drift Y	Stiff Yh	Stiff Y
kN/m	kN	mm	kN	kN/m
6998.624	0	0.0002625		0
8623.651	0	0.0003936		0
7865.807	0	0.001		0
5955.322	0	0.001		0
0	22.1234	8.834		2504.263
0	40.87	11.194		3651.004
0	52.7735	13.998		3769.956
0	58.2495	17.7		3290.888

Figure 10 CSI ETABS Stiffness Results When Subjected to Shear Force

Calculated Values for Math Model:

Through the modal analysis, modal damping ratios can be obtained. Modal damping ratios account for all energy-dissipating mechanisms and help construct the damping matrix, C, by calculating the proportionality coefficients. According to Rayleigh's damping model, for any nth mode,

$$\zeta_n = \frac{\lambda}{2\omega_n} + \frac{\mu\omega_n}{2}$$

Where ζ_n is the damping ratio and ω_n is the modal frequency. Note λ is the mass proportionality while μ is the stiffness proportionality. By selecting any two modes from Figure 8, a system of equations can be created to solve for the two values. Buildings have damping ratios between 2 and 6 percent depending on the age and other factors. Using a damping ratio of 3 percent and the first two modal cases from Figure 8 the proportionalities are,

$$0.03 = \frac{\lambda}{2\omega_1} + \frac{\mu\omega_1}{2}$$

$$0.03 = \frac{\lambda}{2\omega_2} + \frac{\mu\omega_2}{2}$$

Where the selected frequencies are,

$$\omega_1 = 4.7565 \frac{\text{rad}}{\text{s}} \; and \; \omega_2 = 6.7347 \frac{\text{rad}}{\text{s}}$$

Using substitution,

$$\mu = 0.0052 \; and \; \lambda = 0.1673$$

Table 3 Constant Calculations for Model

Variable	Calculation
e_x	1.3589 m
$k_{\theta\theta}$	5.6909× 10^4
$k_{\theta r}$	5.0832× 10^4
ω_θ	0.5566 rad/s
ω_y	0.4088 rad/s
Ω_θ	1.3615
r_g	2.8868 m
μ	.0052
λ	0.1673

Uncontrolled Response:

Two earthquake inputs were retrieved to observe the model response. One is measured in Northern California in Ferndale City Hall on the 6th of June 1960, as shown in Figure 11. The second is also measured in Northern California in Cape Mendocino on the 7th of June 1975, as shown in Figure 12. The test inputs were retrieved from the PEER Ground Motion Database. Raw data was provided as vectors of time against position, velocity, and acceleration for the duration of the seismic measurement in units of gravity. The metric constant of gravity, 9.81 m/s^2, was used to scale the seismic responses.

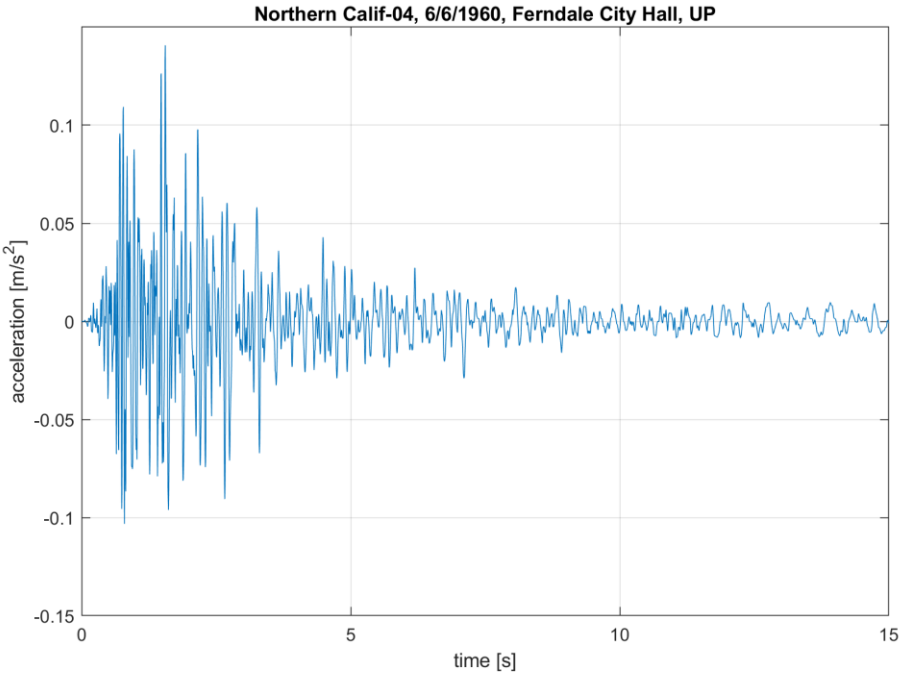

Figure 11 Ferndale City Hall Earthquake Acceleration vs. Time

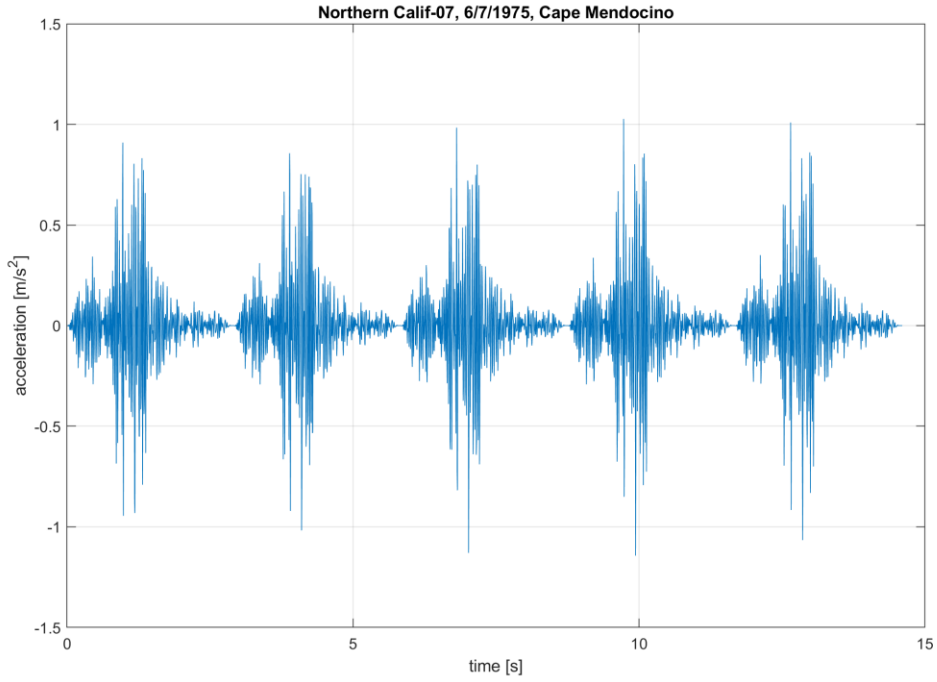

Figure 12 Cape Mendocino Earthquake Acceleration vs. Time

In MATLAB Simulink 2021b, the uncontrolled response to the Ferndale and Mendocino earthquakes were graphed against time as shown in Figure 13 and Figure 14 respectively. Notice the response to the Ferndale City Earthquake, although introducing less force by acceleration, results in greater angular displacements. This is probably because of the continuous duration of the Ferndale earthquake compared to the pulse-like behavior of the Cape Mendocino earthquake. Therefore, the Ferndale City earthquake will be used to observe responses and tune the controller in Chapter 4.

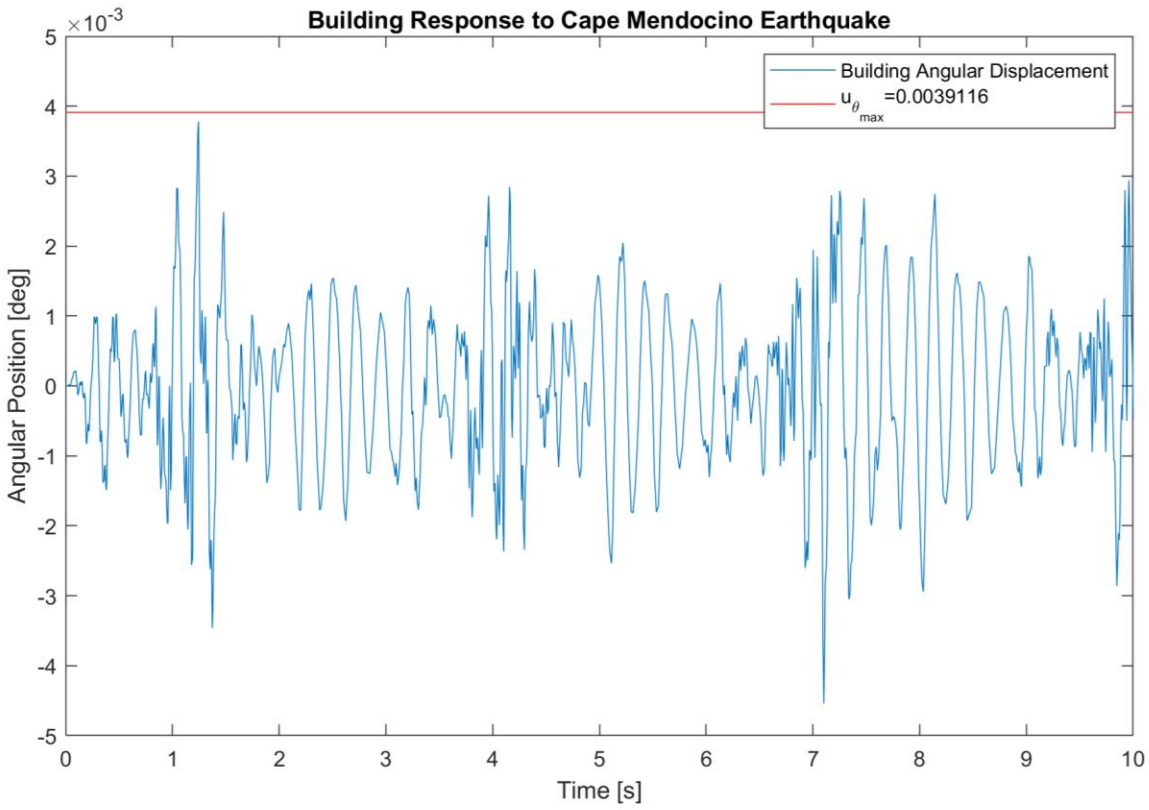

Figure 13 Building Open Loop Response to Mendocino Earthquake in Degrees

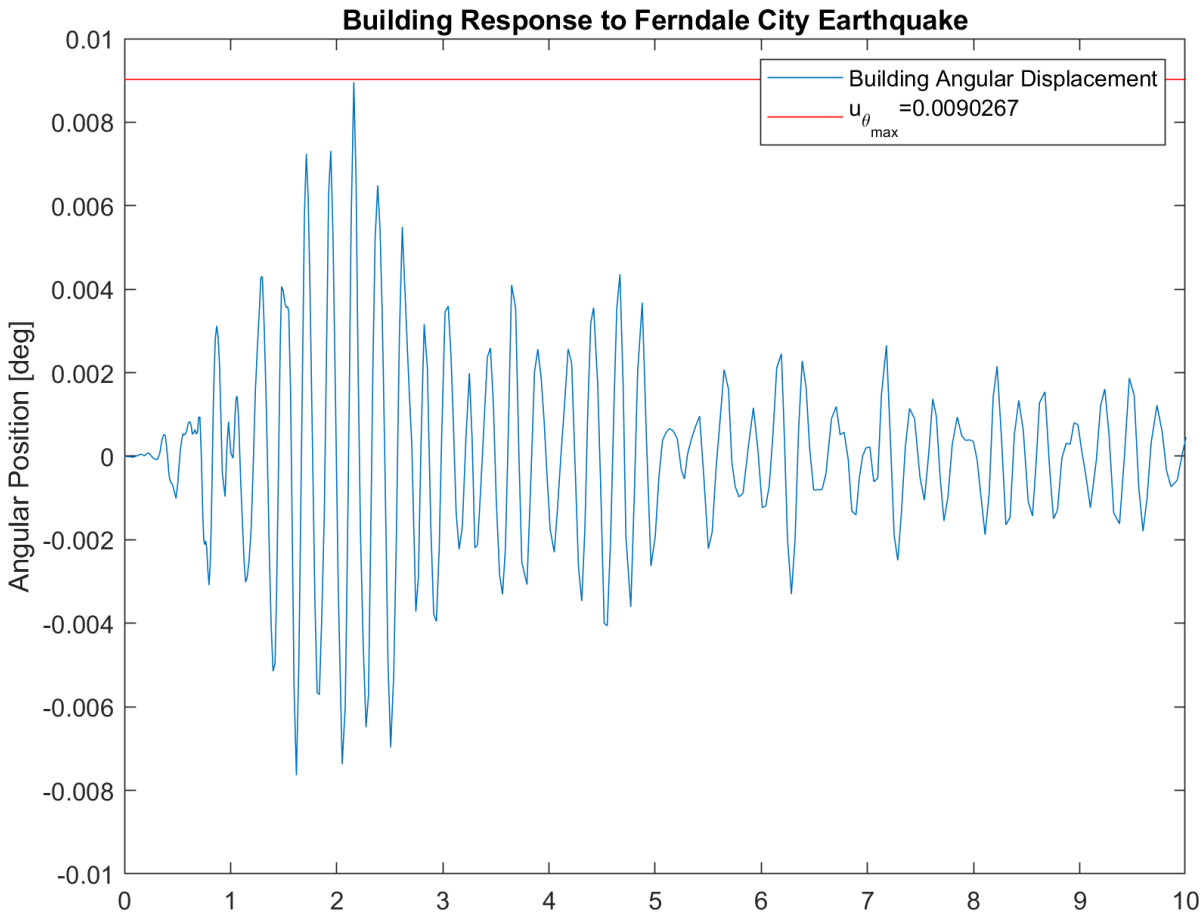

Figure 14 Building Open Loop Response to Ferndale Earthquake in Degrees

Chapter 4: Control Design

Control Theory:

Control theory is necessary to manipulate a system so that it behaves as desired. This is a particularly useful concept when the system must respond to a range of stimuli or when the inputs are hard to predict. For example, earthquakes are difficult to predict and are stochastic. Deciding on a desired output and comparing it to the true output of the system, the error can be used to inform future dynamic behavior. One question is how the system should account for error. As humans, we can translate complex stimuli into endless responses naturally. How can a machine do the same? How does one map out preferred actions for different scenarios?

First, one would want to be able to predict the natural behavior of the system. This was done through defining and formulating equations of motion in Chapter 2. Then, the goal is to find a mathematical rule that influences how the defined system accounts for error. The mathematical rule would dictate changes to what is applied to the system and essentially drive the dynamics of the system to zero error. This mathematical rule is known as the control law,

$$u(t) = Kx(t)$$

The control law states that the desired input $u(t)$ can equal the state of the system $x(t)$ when the state is adjusted by some gain K. In other words, the gain is the value needed to adjust error and reach a desired input.

Different control designs implement different variations of the control law. The feedback control law for LQR in continuous time is defined as,

$$u(t) = -R^{-1}B^{T}Px(t)$$

$$\therefore K = -R^{-1}B^{T}P$$

With a quadratic cost function to take into account the work done,

$$J(x,u) = \int_0^T ((x_t - x_{ref})^T Q(x_t - \mathrm{x_{ref}}) + u^T Ru)dT$$

$$Q = \begin{bmatrix} q_1 & \cdots & 0 \\ \vdots & \ddots & \vdots \\ 0 & \cdots & q_n \end{bmatrix}$$

$$R = \begin{bmatrix} r_1 & \cdots & 0 \\ \vdots & \ddots & \vdots \\ 0 & \cdots & r_m \end{bmatrix}$$

Where the cost J should be minimized over time. R is a positive definite matrix that relates the input $u(t)$ to the cost. In other words, R penalizes the work done by the hydraulic linear actuator. Q is a positive definite matrix that relates error to the cost. Greater Q values penalize error in each state. Note B comes from the state space representation of the linear model. Finally, P is the solution to the cost function and is an algebraic Ricatti equation,

$$A^T P + PA - \mathrm{PBR^{-1}}B^T P + Q = 0$$

This equation is nonlinear and could be solved by hand. However, this project uses the lqr() function in MATLAB 2021b to solve for gain K. In summary, LQR takes a linearized dynamic system, the desired output of the state variables, known as the reference state, and tries to minimize the cost function. Even if the theoretical model of the system is not perfect, as linearizing dynamics and certain ideal assumptions tend to create uncertainty, the mathematical rule should still work to reach optimal control. How does one define optimal? These are numerical, measurable parameters of the desired response. They are the goal posts of control design. Zero error is ideal but often not realistic. For the seismic control system, the best response would be zero movement from the building, but the preferred response would be to reduce peak rotational displacement by 50 percent.

There are also constraints such as the maximum force of the hydraulic linear actuator, or the max flow rate the servo valve can produce. The initial conditions are assumed to be zero because the building should be at a resting state before seismic excitation. These parameters and constraints can also be justified by restrictions in the environment or a desire to mimic the performance of another system. Buildings cannot sway beyond a certain point because they will incur damage or cause damage to surrounding areas. In this project, 50 percent peak reduction was chosen as a comparable performance to other control systems described in the literature review. The summary of preferred response parameter is in

Table 4. In addition, LQR is a form of full-state feedback and requires a controllable system. The controllability of the system can be verified if the rank of its controllability matrix is equivalent to the number of states. This was verified with the MATLAB function ctrb(), which calculated the controllability matrix from A and B, and rank() , which calculated the rank from the controllability matrix.

Table 4 Preferred Response Parameters

Parameter	Value
Reduce Peak Angular Displacement u_θ	≥50%
Initial Control Response Delay	<1 second

Two key parameters were chosen. Peak displacement reduction is based on the successful performance of similar systems and the time response is set based on observations on the general behavior of earthquake data, which require a very responsive system.

MATLAB SIMULINK Controller Simulations:

The controller design was implemented in MATLAB Simulink 2021b as pictured in Figure 15 where the calculated gain is under the gain block labeled,' LQR Gain' and produces a control response R(s). The decimation of time was set to 1 millisecond with a run time of 15 seconds, except for Figure 21 which was run for 1 second.

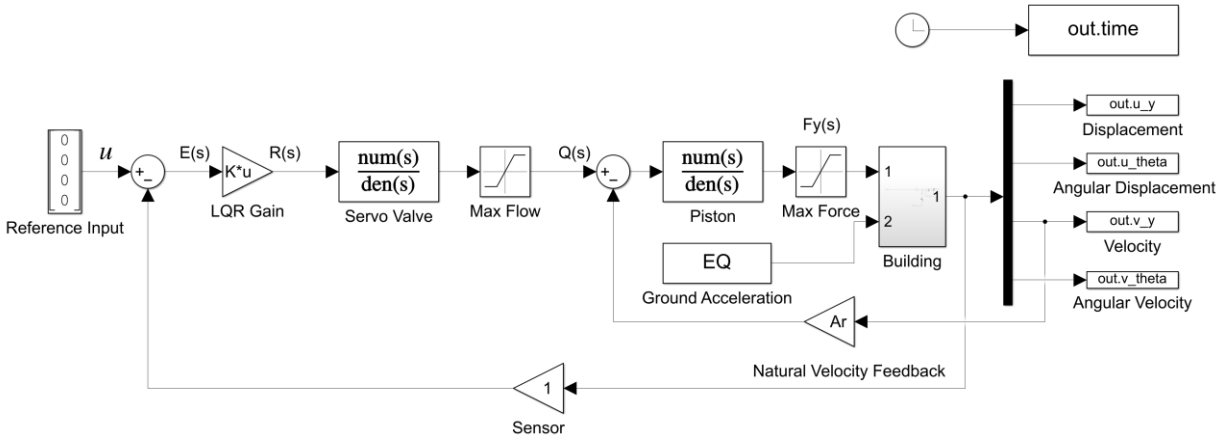

Figure 15 MATLAB Simulink Diagram with LQR Control Design

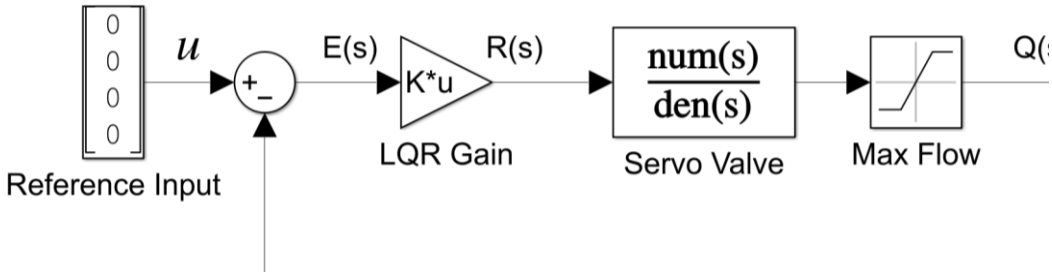

Figure 16 Close View of LQR Gain from Figure 15

For the cost function, Q is a 4x4 matrix that multiplies against the error of four states and R is an integer value that multiplied by the input to the servo valve. This project is

specifically concerned with torsional damage and aims to reduce torsion. Therefore, only torsional error will be penalized by some factor Q_2 at position Q(2,2) to correlate with u_θ that is also in position 2 of the state variable matrix Z**,** as defined in Chapter 2,

$$Q = \begin{bmatrix} 0 & 0 & 0 & 0 \\ 0 & Q_2 & 0 & 0 \\ 0 & 0 & 0 & 0 \\ 0 & 0 & 0 & 0 \end{bmatrix}$$

The effort of the actuator is not of great concern but does have limits in its capabilities that it should not realistically exceeded. Therefore,

$$\mathrm{R} \leq 1.$$

Additional system parameters that will be simulated are the error in the estimate for center of rigidity and the offset of the actuator from the center of mass. As the center of mass was determined to be at 4.51 meters from the flexible edge of the floor plan,

$$0 < d < 4.51\ m$$

Rotational Response with Increasing Q_2:

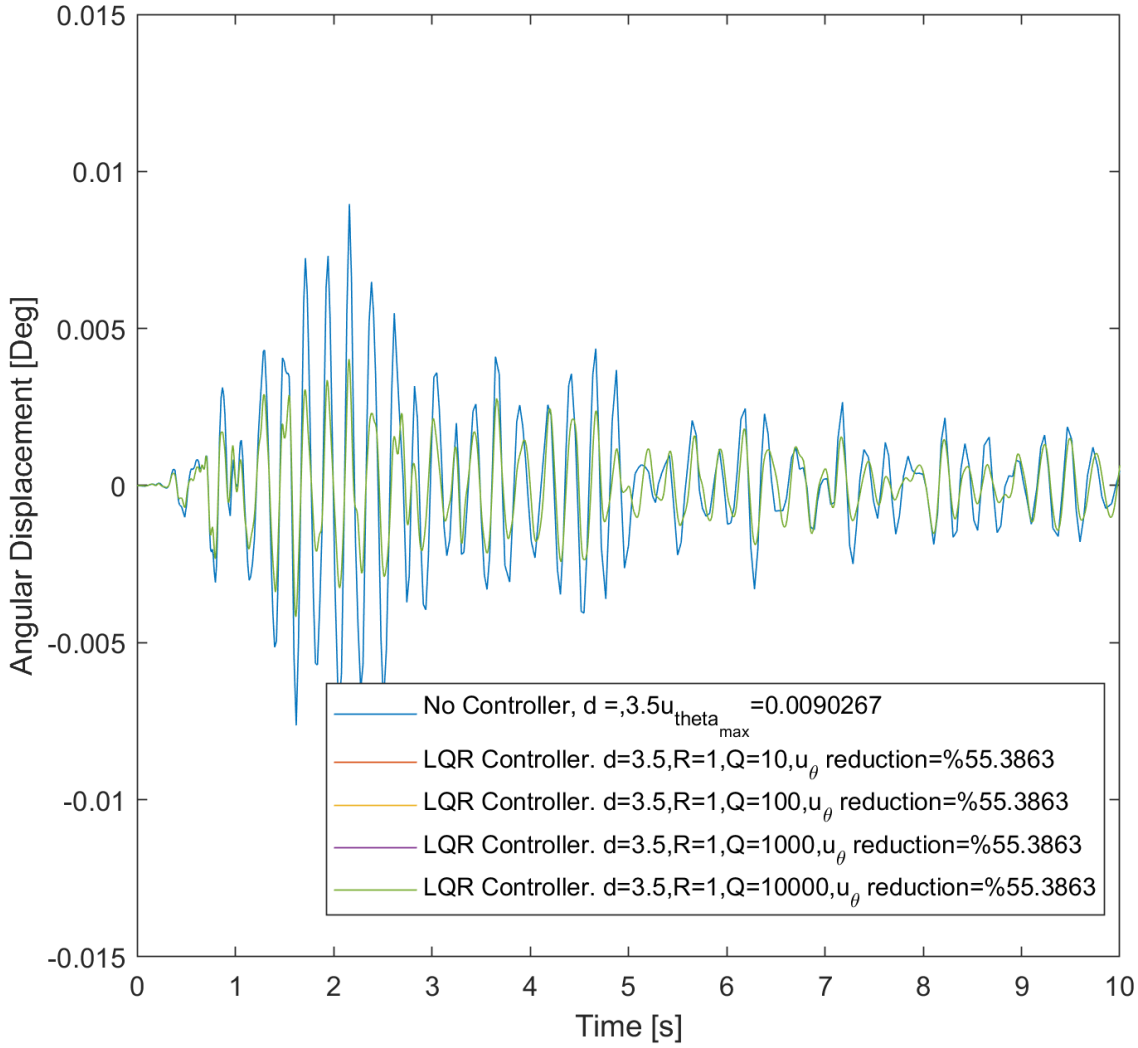

Figure 17 Rotational Response with Increasing Q in LQR controller

Rotational Response with Increasing R:

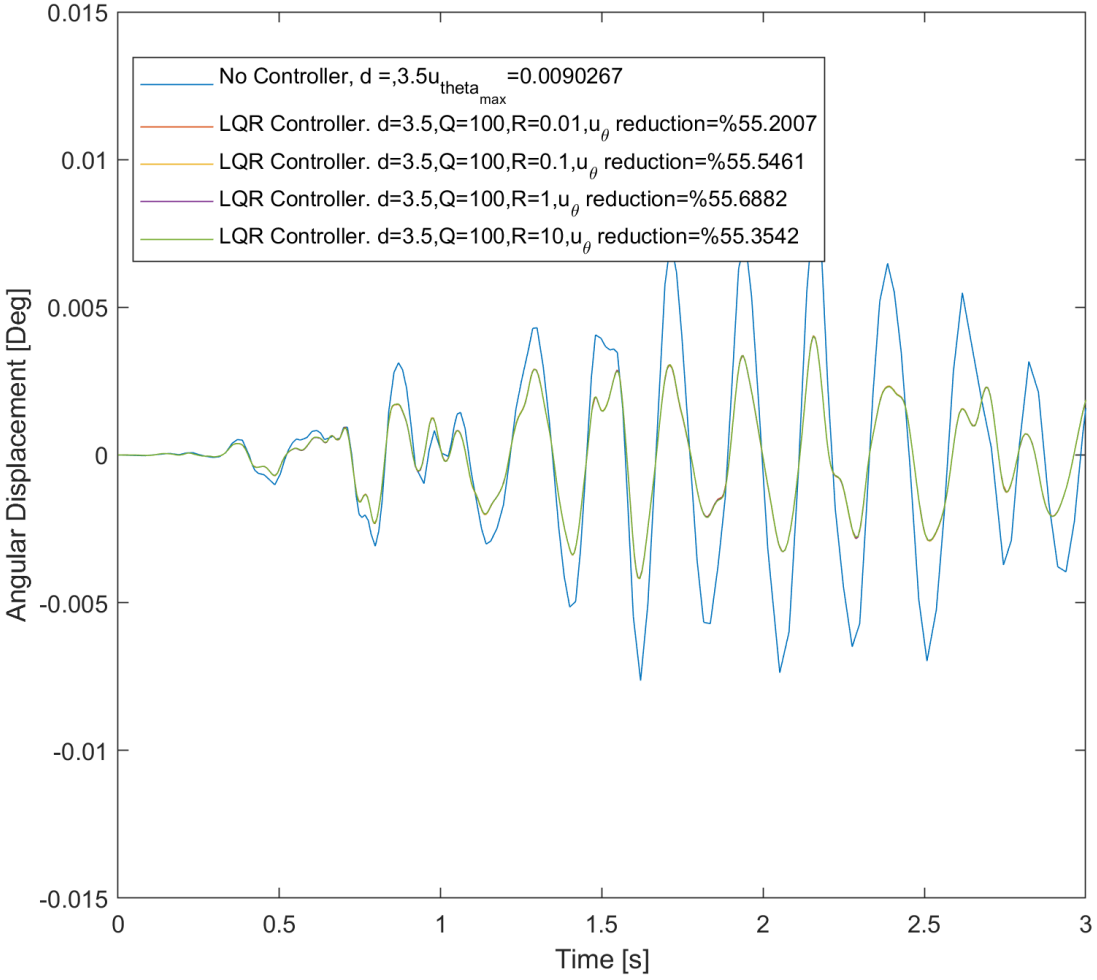

Figure 18 Rotational Response with R ≤ 1 in LQR Controller

Rotational Response with Increasing Actuator Offset, d:

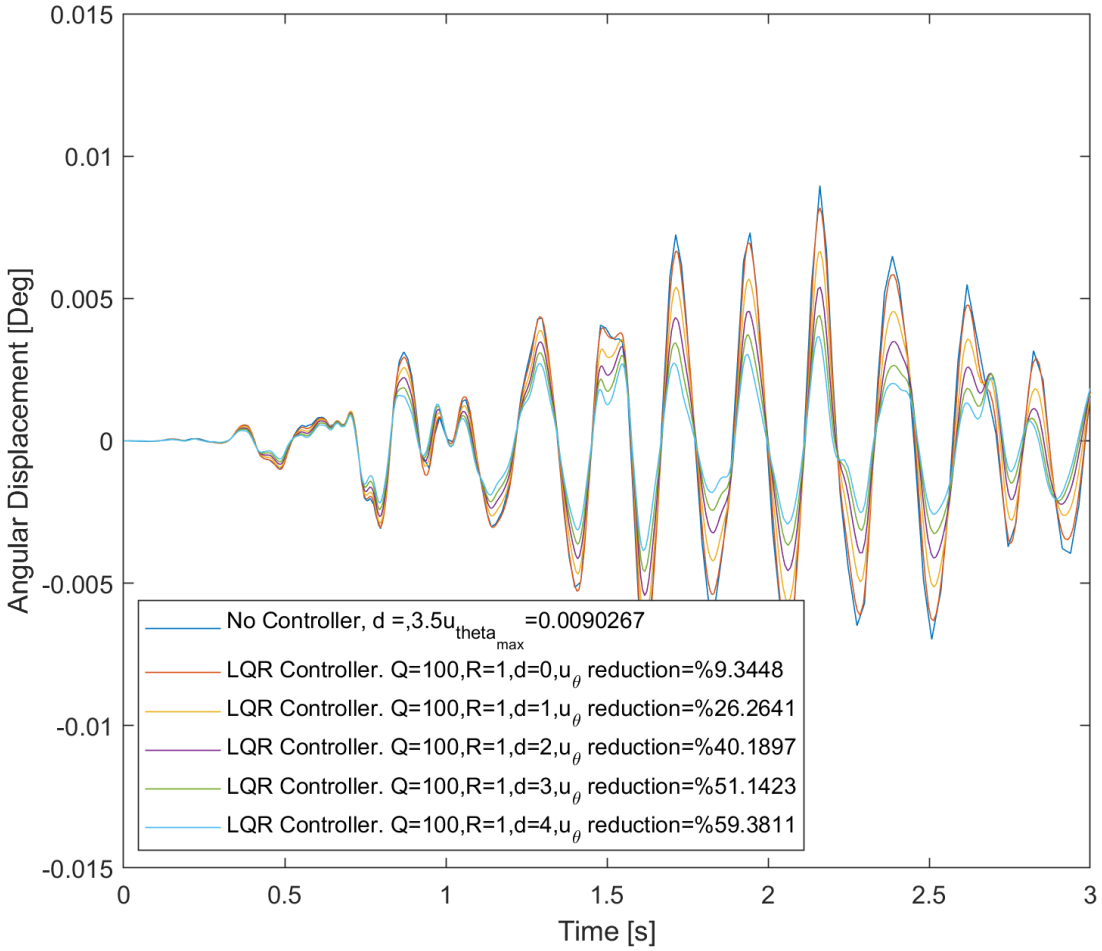

Figure 19 Rotational Response Increasing Actuator Offset, d, with LQR Controller

Lateral Response with Increasing R:

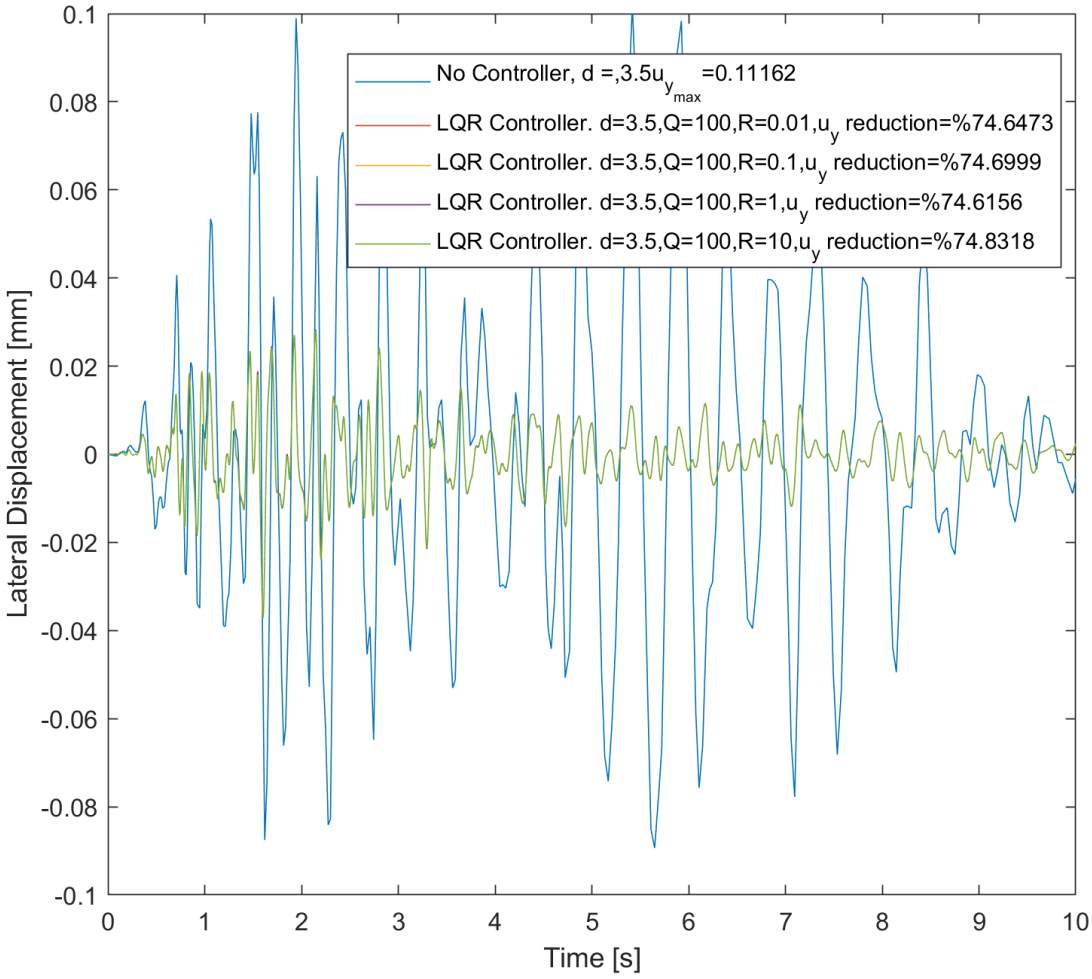

Figure 20 Lateral Response with Increasing R in LQR Controller

Rotational Response within 1 second:

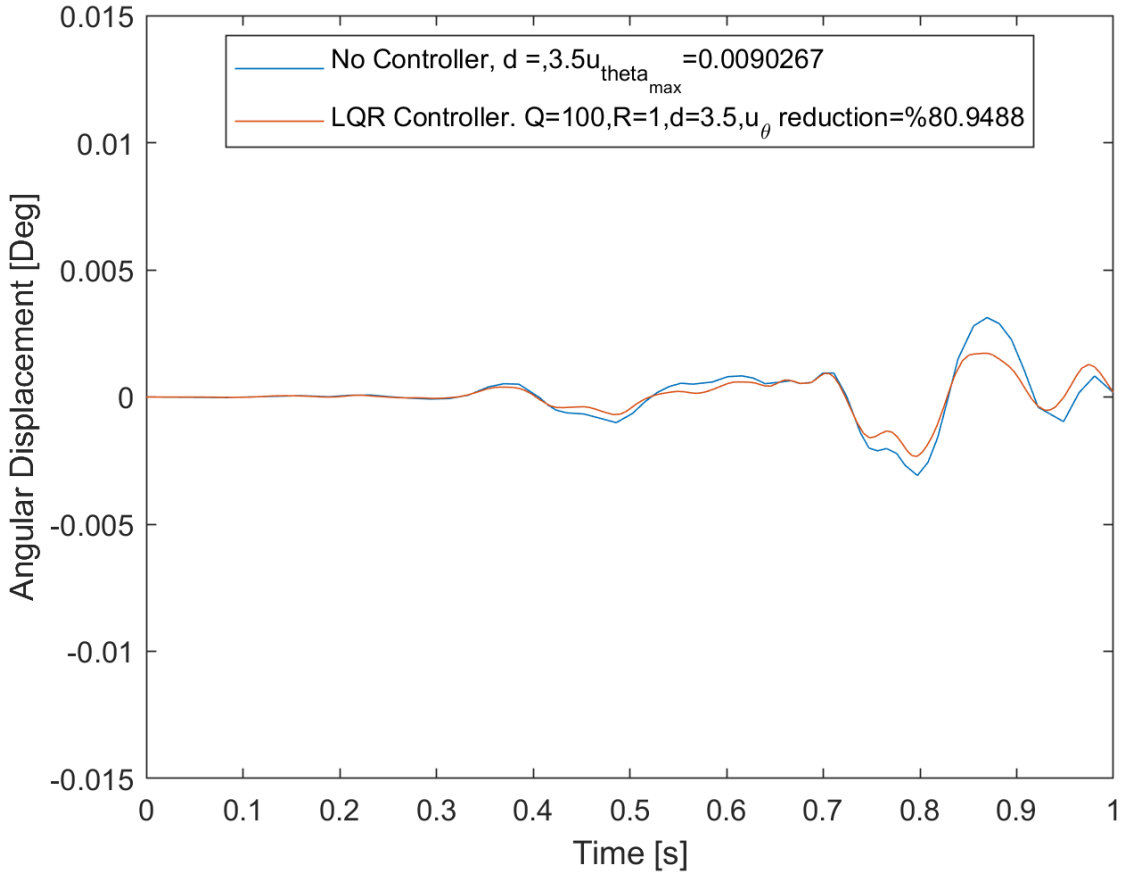

Figure 21 Rotational Response within 1 second in LQR Controller

Effect of Intentional Error on Center of Rigidity:

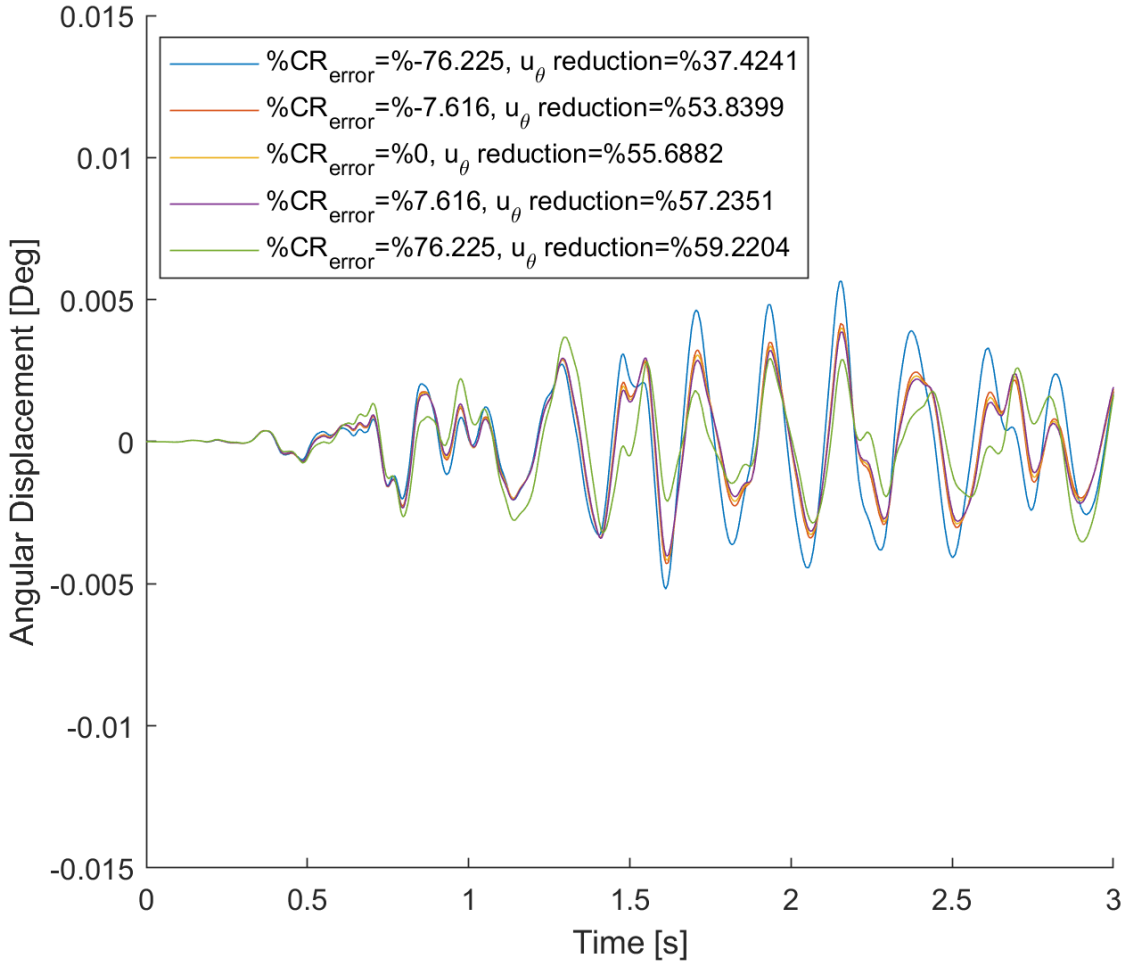

Figure 22 Effect of Center of Rigidity on LQR Control

Chapter 5: Discussion

To tune the LQR controller, the building response was simulated over a range of gains calculated from a range of Q_2 values, which is denoted simply as Q in the simulation plots. This Q value penalizes the rotational response of the building and was expected to reduce the peak angular displacement as desired. In Figure 17, only two lines are distinguishable. The uncontrolled response is in blue and the controlled responses in green. Ranging from 10 to 10,000, all Q values produced a 55 percent reduction in peak angular displacement. The response was assessed at extremely high Q values to verify the controller was adjusting to the variables. The extreme values did alter the response by fractions of a percent. A %55 percent reduction was about as high as the response would perform before becoming less preferable. Therefore, Q was selected to be 100 as it resulted in at least a 50 percent peak reduction. One relationship observed was that a high Q value, such as 10^{20}necessitated a larger R value or the response would become unstable. This relates to how the cost function attempts to find a balance between actuator effort and reducing error and Q was over-emphasized at the expense of the actuator.

$$Q = \begin{bmatrix} 0 & 0 & 0 & 0 \\ 0 & 100 & 0 & 0 \\ 0 & 0 & 0 & 0 \\ 0 & 0 & 0 & 0 \end{bmatrix}$$

Next, a range of R values was evaluated with the selected Q and plotted in Figure 18. Slight variation was observed, and all responses remained around 55 percent. When R is 1 the response has the highest reduction. This is a tenth of a percent more than other tested R values. Therefore, R was set as one,

$$R = 1$$

A third feature of the system is the offset of the actuator from the center of mass. More offset should introduce a higher torque with less effort on the hydraulic linear actuator. The response was predicted to improve with larger offset. This held true when plotted in Figure 19. Surprisingly, the system was more sensitive to the change in offset than any of the control values. Unlike Figure 17 and Figure 18, the varying parameters have distinguishable results. Note zero offset produces about a 9 percent reduction in rotation. This is reasonable because the rotation and translation of the building are coupled responses. If one reduces so should the other by some amount. In this case, even without targeting rotation directly, any seismic control system using linear forces can reduce torsion to some extent. An offset of 4 meters minimized the response an additional 4 percent from the previous simulations. With the preferred response of at least 50 percent, an offset of 3.5 meters was selected as an adequate placement.

Figure 20 illustrates how the chosen controller specifications reduce lateral displacement. Although this was not the focus of the control design, approaching error from the perspective of rotation resulted in a about 74% reduction in peak lateral displacement. Again, adjusting a range of R values did not significantly influence the amount of lateral displacement reduction.

To address the performance parameter of having an initial delay below 1 second, the chosen LQR specifications (Q=100, R=1) was run for only 1 second. The peak reduction was about 80 percent within this timeframe and fulfills the desired parameter. The LQR controller actually becomes less effective as the earthquake develops when comparing the 1 second simulation to the 15 second simulations.

A final question to address is how the accuracy of the center of rigidity affects the control response. The center of rigidity, among other structural properties, is a difficult value to derive because it requires an intimate knowledge of the specific structure of interest. An error was added to the position of the eccentricity value. As shown in Figure 22, a 7 percent underestimate and 7 percent overestimate each resulted in a 2 percent difference from the initial performance of the controller. A 76 percent underestimate resulted in an 18 percent difference in response while a 76 percent overestimate resulted in a 4 percent difference. Underestimation deteriorates the performance of the controller more than overestimation.

References List

Alipour, A., & Zareian, F. (2008, October). Study Rayleigh damping in structures; uncertainties and treatments. In the 14th world conference on earthquake engineering (pp. 12-17).

Baygi, S. M. H., & Karsaz, A. (2018, March). A hybrid optimal PID-LQR control of structural system: a case study of salp swarm optimization. In 2018 3rd Conference on Swarm Intelligence and Evolutionary Computation (CSIEC) (pp. 1-6). IEEE.

Botis, M. F., & Cerbu, C. (2020). A Method for Reducing of the Overall Torsion for Reinforced Concrete Multi-Storey Irregular Structures. Applied Sciences, 10(16), 5555.

Braz-César, M. T., Folhento, P. L., & Barros, R. C. (2018, June). Numerical Simulation of Torsional Response Control of a Plan-Eccentric Mass Distribution Building by Using Magnetorheological Dampers. In 2018 13th APCA International Conference on Automatic Control and Soft Computing (CONTROLO) (pp. 358-363). IEEE.

Buckle, I. G. (2000). Passive control of structures for seismic loads. Bulletin of the New Zealand Society for Earthquake Engineering, 33(3), 209-221.

DeSilva, C.W. (1989), Control sensors and actuators, Prentice Hall, Inc., Englewood Cliffs, N.J.

Fisco, N. R., & Adeli, H. (2011). Smart structures: part I—active and semi-active control. Scientia Iranica, 18(3), 275-284.

Hudnut, K.W., Wein, A.M., Cox, D.A., Porter, K.A., Johnson, L.A., Perry, S.C., Bruce, J.L., and LaPointe, D., 2018, The HayWired earthquake scenario—We can outsmart disaster: U.S. Geological Survey Fact Sheet 2018–3016, 6 p., https://doi.org/10.3133/fs20183016.

(ICC), I. C. C. 2015 International Residential Code (IRC): ICC Digital Codes. 2015 INTERNATIONAL RESIDENTIAL CODE (IRC) | ICC DIGITAL CODES. Retrieved April 27, 2022, from https://codes.iccsafe.org/content/IRC2015

Kijewski, T., & Kareem, A. (2000). Estimation and modeling of damping and engineering auxiliary damping systems in civil engineering structures: an overview. NatHaz Modeling Laboratory Report, 9.

Lee, C. L., & Wang, Y. P. (2004). Seismic structural control using an electric servomotor active mass driver system. Earthquake engineering & structural dynamics, 33(6), 737-754.

Mahini, S. S., Setunge, S., & Hadigheh, S. A. (2015). Performance vs resilience-based earthquake design for low and medium-rise retrofitted RC buildings. In Proceedings of the Tenth Pacific Conference on Earthquake Engineering Building an Earthquake-Resilient Pacific (PCEE2015), Sydney, Australia.

Mehana, M. S., Mohamed, O., & Isam, F. (2019, September). Torsional behaviour of irregular buildings with single eccentricity. In IOP Conference Series: Materials Science and Engineering (Vol. 603, No. 5, p. 052028). IOP Publishing.

Mevada, S. V., & Jangid, R. S. (2012). Seismic response of torsionally coupled system with magnetorheological dampers. Advances in Civil Engineering, 2012.

Nie, X., Zhang, S., Jiang, T., & Yu, T. (2020). The strong column–weak beam design philosophy in reinforced concrete frame structures: A literature review. Advances in Structural Engineering, 23(16), 3566-3591.

Özmen, G., Girgin, K., & Durgun, Y. (2014). Torsional irregularity in multi-story structures. International Journal of Advanced Structural Engineering (IJASE), 6(4), 121-131.

Villaverde, R., & Koyama, L. A. (1993). Damped resonant appendages to increase inherent damping in buildings. Earthquake engineering & structural dynamics, 22(6), 491-507.

Yamazaki, S., Nagata, N., & Abiru, H. (1992). Tuned active dampers installed in the Minato Mirai (MM) 21 Landmark Tower in Yokohama. Journal of Wind Engineering and Industrial Aerodynamics, 43(1-3), 1937-1948.

Yan, X., Xu, Z. D., & Shi, Q. X. (2020). Fuzzy neural network control algorithm for asymmetric building structure with active tuned mass damper. Journal of Vibration and Control, 26(21-22), 2037-2049.

Conclusions and Looking Forward

The project began with an idea on how to improve my senior design project and expanded into a full exploration of control theory and seismic engineering. General conclusions on the dynamic behavior of the system are that overestimation of certain properties should not significantly impact the LQR control performance. This relates to the robust approach of an LQR controller. The design strategy in the project varies from the literature reviewed in that the control design was purely about the torsional response. Nevertheless, the accompanying reduction in lateral translation was comparable to real documented systems. General improvements on the control system include the accurate modelling of a sensor such as an accelerometer. The LQR design could be expanded into an LQG design with a Kalman filter to address the ground disturbance as noise. The LQR design did not take this into account in its control law. Additional inputs should be tested. Hundreds of data sets are available from the PEER Ground Motion database. Looking forward, the techniques of control design applied in this context would be valuable to explore in other fields. Active seismic control overall was a unique challenge to address and will hopefully become more relevant in the United States in coming years.

Figures

Appendix

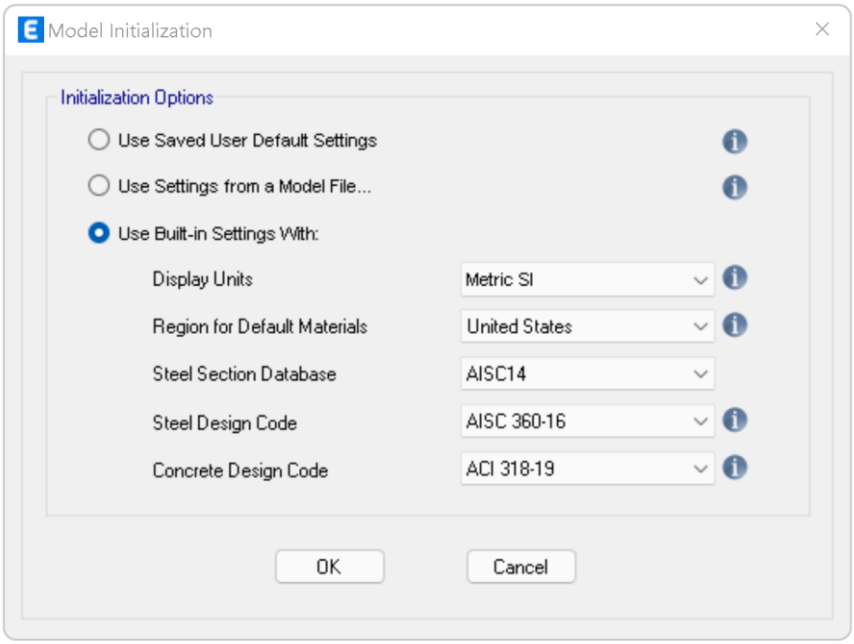

Figure 23 Step 1: CSI ETABS New Model Set Built-In Settings

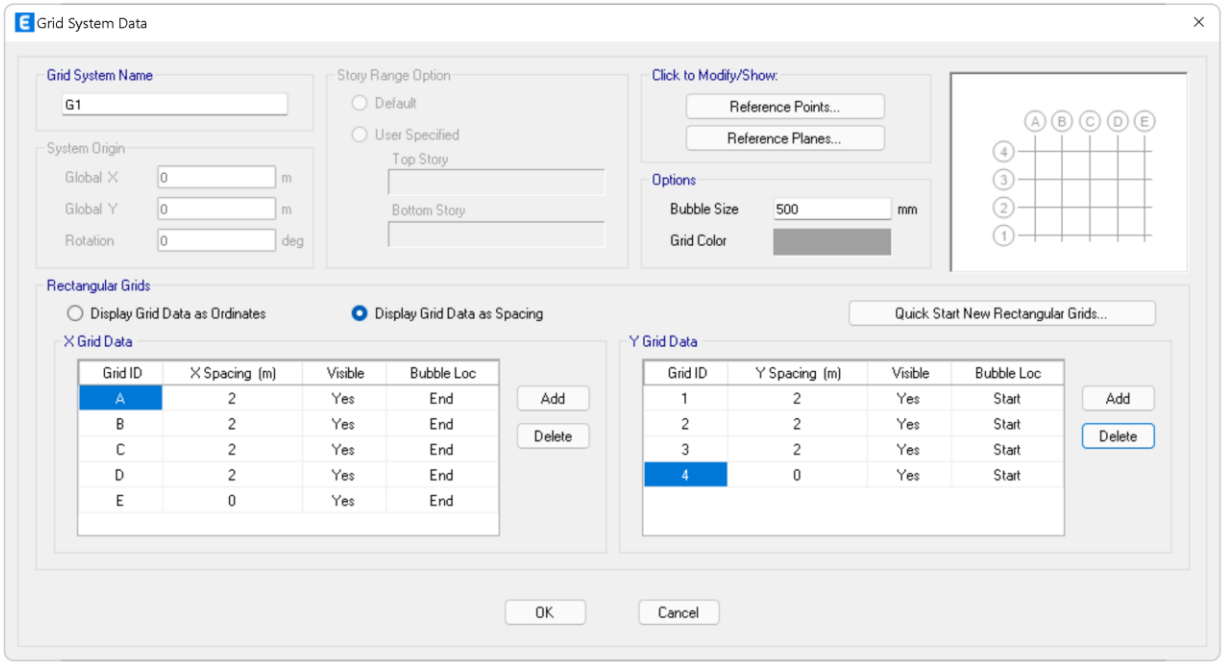

Figure 24 Step 2: Assign Layout According to Layout in Chapter 1

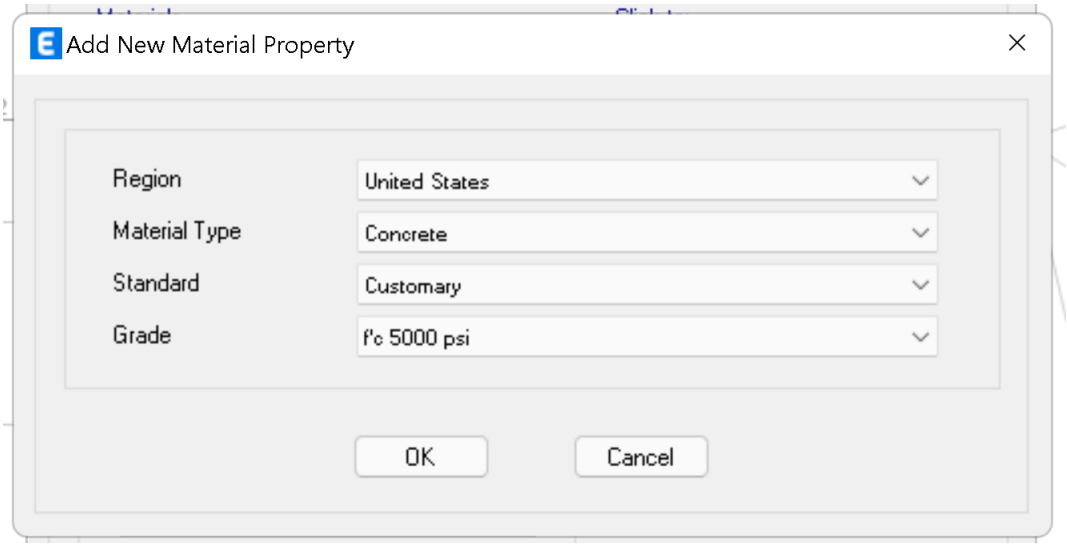

Figure 25 Step 3. Create Concrete Material

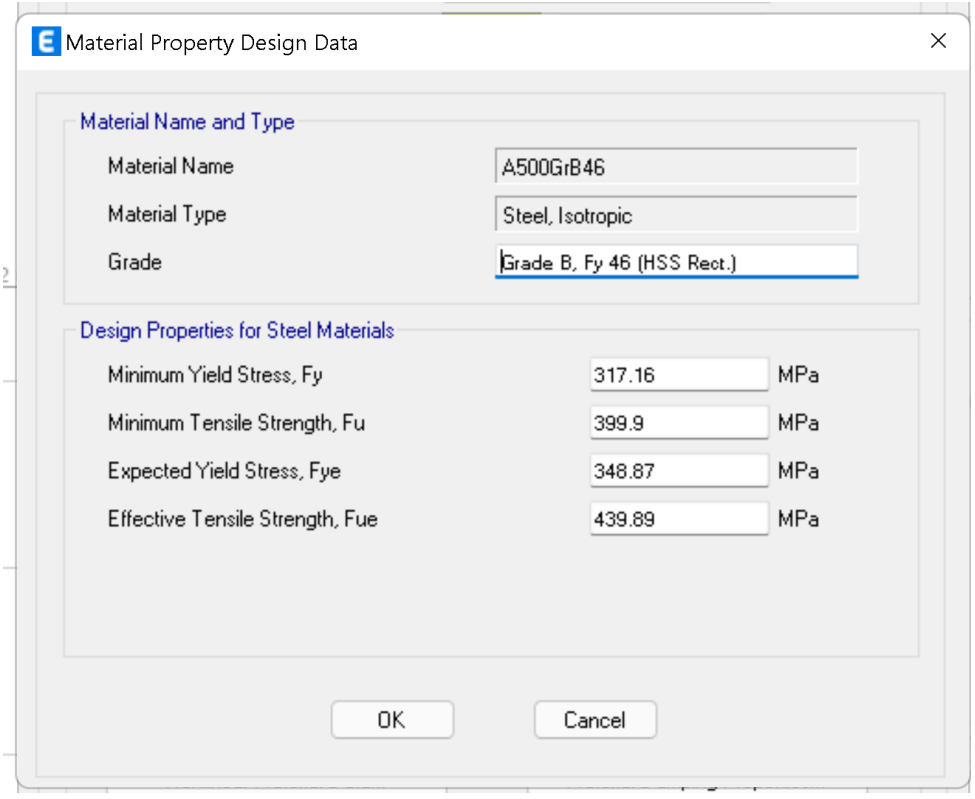

Figure 26 Step 4: Create Steel Material

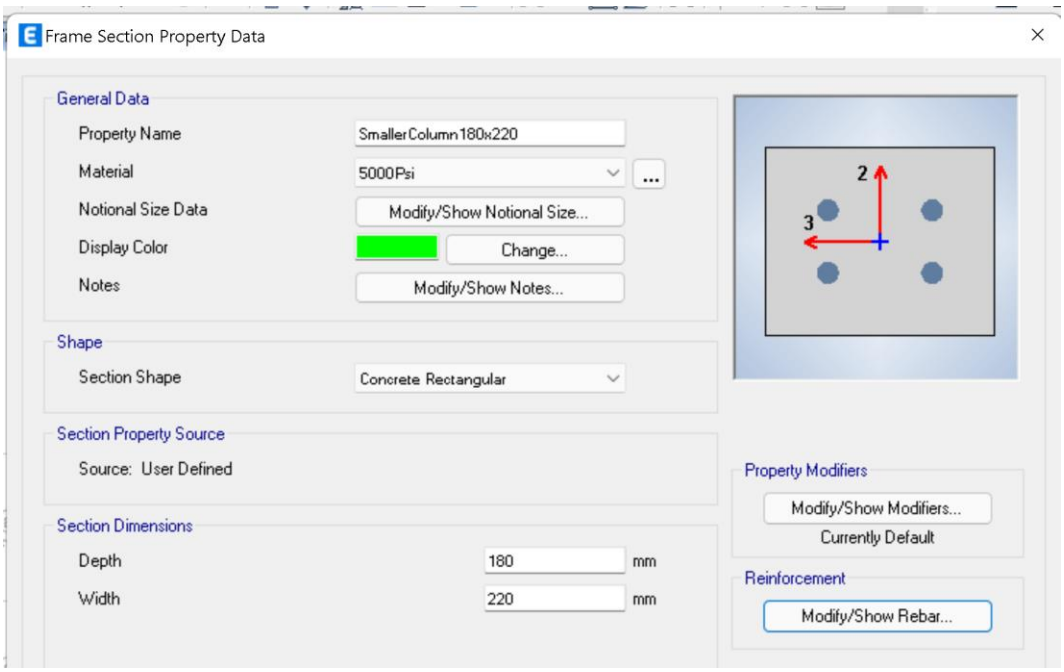

Figure 27 Step 5: Create RCC Element of Small Column

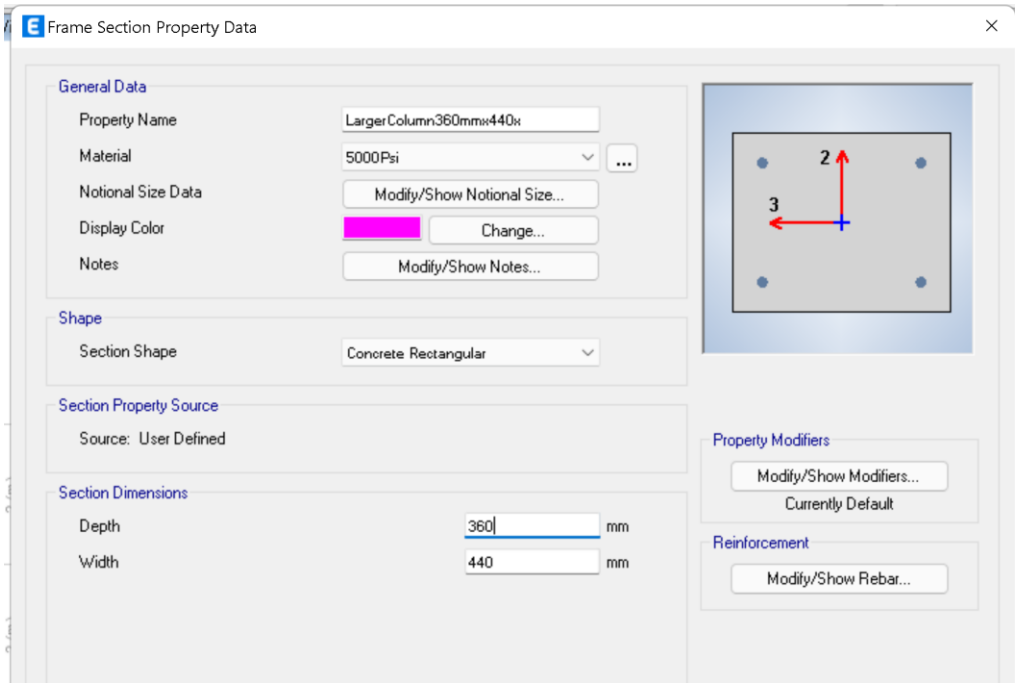

Figure 28 Step 6: Create RCC Element of Large Column

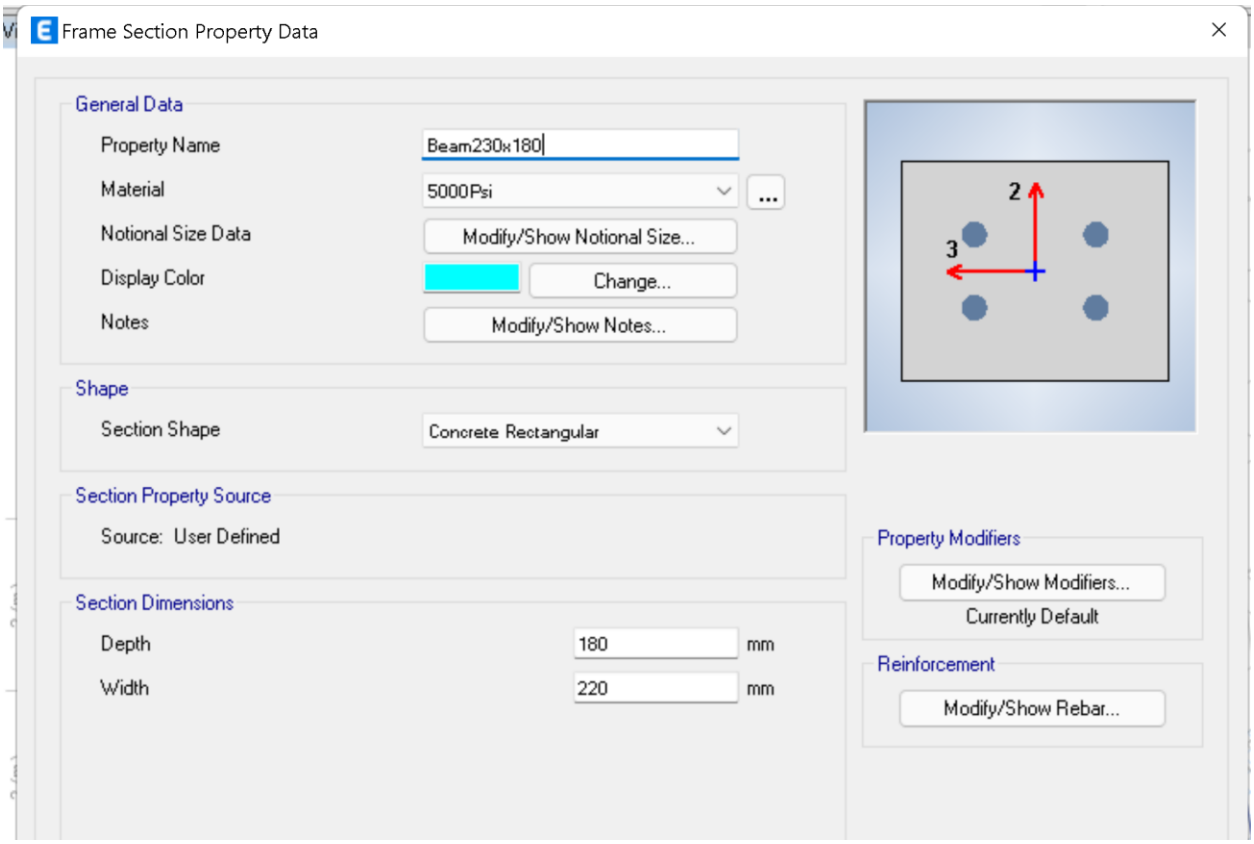

Figure 29 Step 7: Create a RCC Beam Element

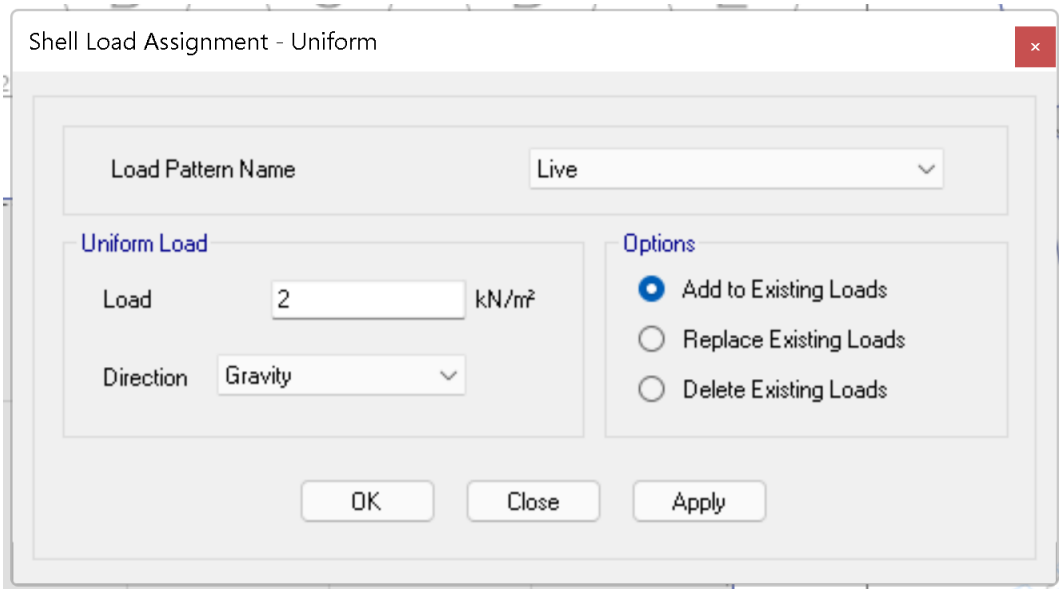

Figure 30 Step 8: Assign Live Loads

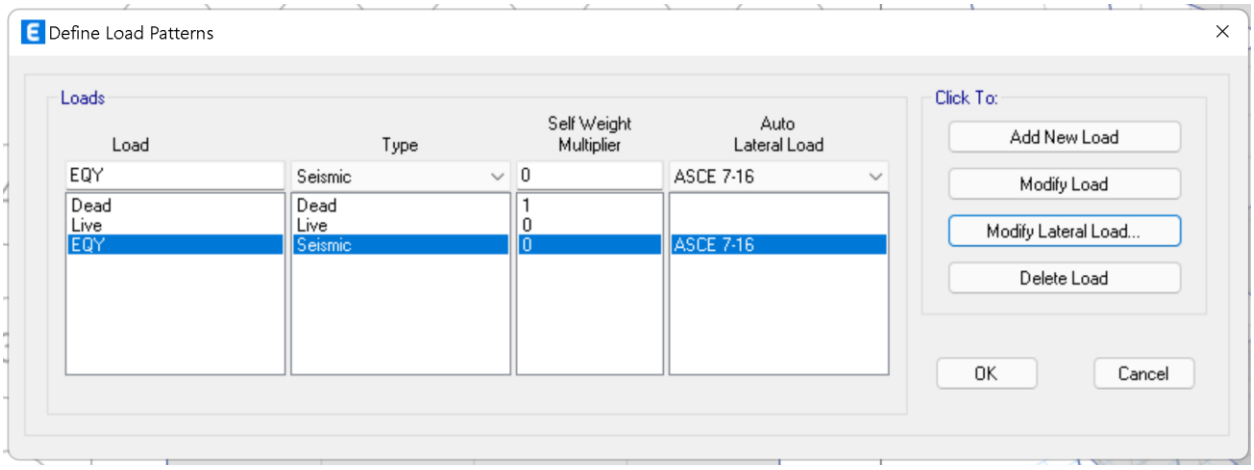

Figure 31 Step 9: Create a Seismic Load

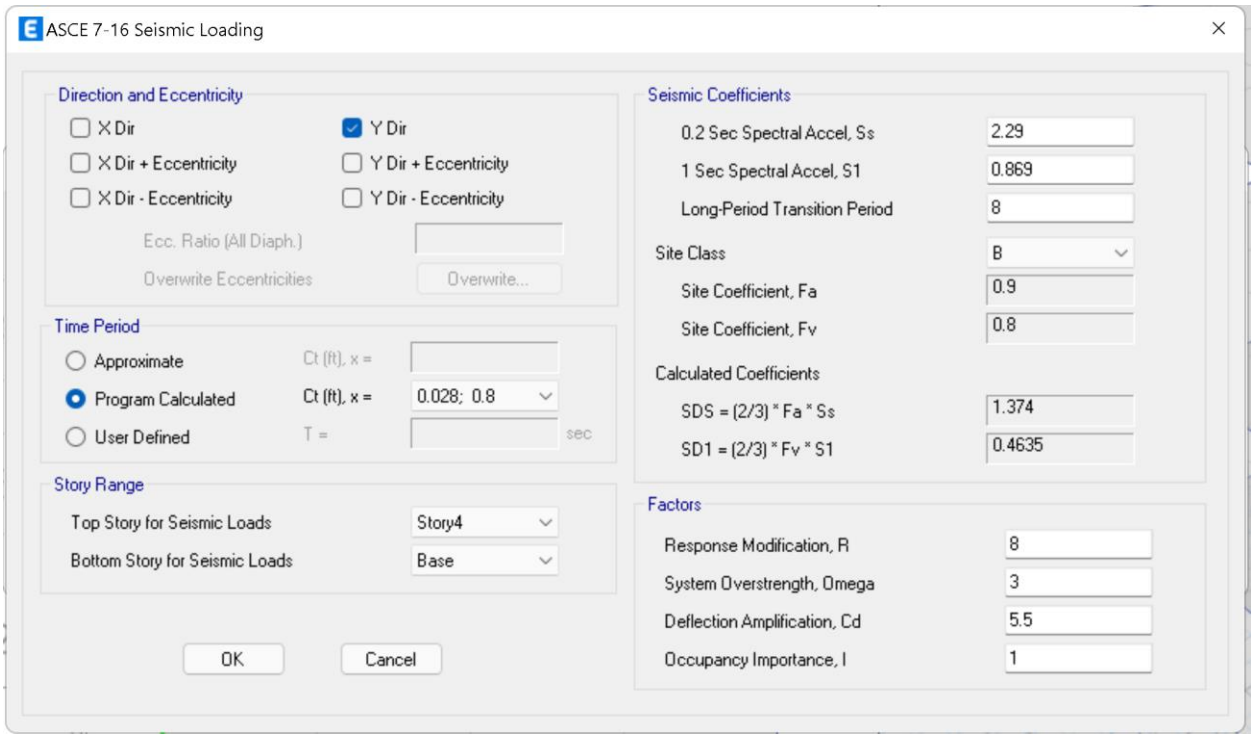

Figure 32 Step 10: Restrict the Seismic Load in the y Direction

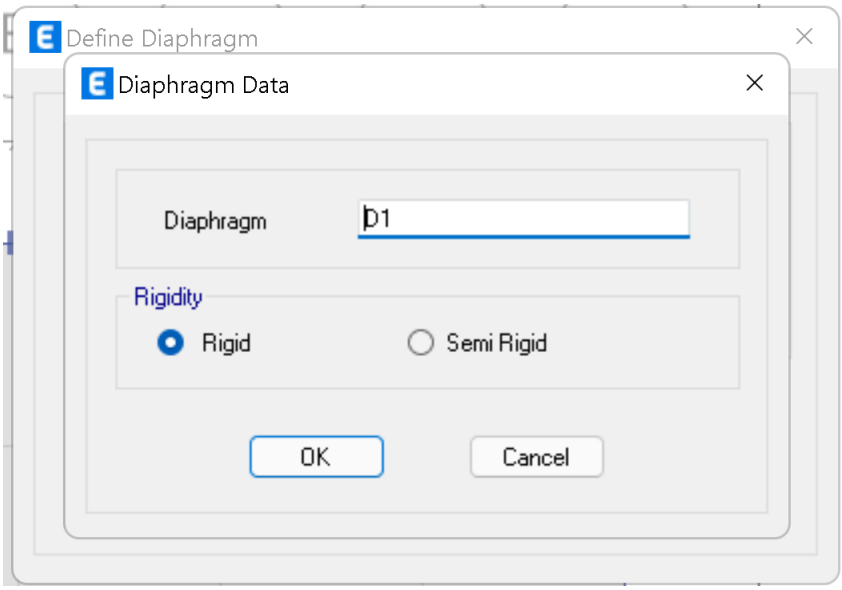

Figure 33 Step 11: Set the Structure as Rigid Body